

6 Viscoelastic Characterisation of Gum Rubber

6.1 Introduction

In the previous chapters the processability of gum rubber was related to its behaviour at large deformation and fracture. A given rubber has a unique deformational behaviour, which may be characterised by its viscoelastic properties. The latter is, in turn, related to the molecular architecture. Therefore, viscoelastic properties play a central role in relating polymerisation conditions to processability of gum rubber. The viscoelastic characterisation has particular importance for gum rubbers, because many of them contain an insoluble fraction called ‘gel’, which makes solution-based characterisation inapplicable.

In this chapter, a development of the viscoelastic characterisation method is described. It begins with methods of describing deformation behaviour, subsequently a treatment of non-linear viscoelasticity is presented. Finally, by using the viscoelastic characterisation method, the processability of gum rubber is related to its molecular architecture.

6.2 Methods of describing deformation

When the subject of deformation of rubber is considered, a conventional approach such as shear or elongation is accepted. The definition of steady state viscosity is an example of the former and that of tensile testing is an example of the latter. However, the deformation of rubber during mixing is not completely shear nor elongation. Therefore, the way to describe this deformation needs to be examined. The bulk compression need not be considered, because rubber is practically incompressible.

For simplicity, consider an elastic body which is in isolation. The deformation of this body may be described by the stress tensor σ_{ij} and the deformation tensor ϵ_{ij} as:

$$\sigma_{ij} = \sum a_{ij} \epsilon_{ij} \quad (6.1)$$

where the subscripts i and j are for the 1, 2, and 3 directions, in orthogonal co-ordinate systems and a_{ij} s are moduli, [1]. Equation 6.1 represents nine equations and is very

complex. Rubber being an isotropic and amorphous body, the relationship may be simplified to only simple shear, σ_{12} , and normal stress components σ_{11} , σ_{22} , and σ_{33} . For an infinitesimal deformation, the shear modulus G and elongational modulus E are related as:

$$G = \frac{E}{2(1+\nu)} \quad (6.2)$$

where ν is Poisson's ratio and equal to 0.5 for rubber:

$$E = 3G \quad (6.3)$$

When Equation 6.3 holds, either shear or elongational measurements need to be performed to adequately describe the rubber behaviour. However, this is limited to infinitesimal deformation.

For describing a finite deformation, a concept of strain energy function is introduced instead of stress, because energy is the basic quantity and stress is the phenomenological expression for the energy change resulting from deformation. The expression for strain takes a strain invariant form. This is based on the understanding that strain should not depend upon a particular choice of coordinate system. Also, the coordinate axis may be rotated from that before deformation to that after deformation. This enables any deformation to be described with strains in three principal axes only. In order for this to be possible, the body must be isotropic and uniform. Therefore, it is not applicable to compounds containing filler. Also, for the rotation of the axis not to alter the magnitude of strain, the body must be isolated. For interconnected elements in finite element analysis, the rotation of the axis may affect the strain in the neighbouring elements. The final derivation of the above theory [2] is presented in the following form for strain energy U :

$$U = \sum_{i=0, j=0} C_{ij} (I_1 - 3)^i (I_2 - 3)^j \quad (6.4)$$

where C_{ij} is a material constant, I_1 and I_2 are strain invariants. In this case $I_3 = 1$ because rubber is practically incompressible. When Equation 6.4 is applied to extensional deformation, the following equation is often used:

$$U = C_1(I_1 - 3) + C_2(I_2 - 3) \quad (6.5)$$

This equation is called the Mooney [3] or Mooney-Rivlin equation.

Although Equation 6.5 is derived through rigorous logic, it is based on a number of premises. Therefore, before applying it to the system of interest, we need to examine if a given case is in conformity with the premises. The equation assumes an equilibrium, and therefore it applies to a crosslinked network only. As gum rubbers are uncrosslinked, they do not attain equilibrium because of the slipping of entanglements. Even with a network, the large deformation data progressively deviate from the form given by the equation.

There is another approach which uses the concept of strain energy and principal strains only; it is called the Valanis-Landel equation [4]. It assumes that the total strain energy may be subdivided into those corresponding to each of three principal strains:

$$u(\lambda_1, \lambda_2, \lambda_3) = u(\lambda_1) + u(\lambda_2) + u(\lambda_3) \quad (6.6)$$

Where λ_1 , λ_2 , and λ_3 are strains expressed as the elongational ratios in the direction of the principal axes. This equation assumes that $u(\lambda_1)$, $u(\lambda_2)$, and $u(\lambda_3)$ may in general take different values; this means the coordinate axes are fixed and are not free to be chosen. This is more like the usual shear and elongational measurements where the magnitude of strain is tied to a specific coordinate system. The concept of strain invariance is not used.

Ogden's equation [5] may be regarded as a specific form of Equation 6.6:

$$u(\lambda_i) = (\mu_i / \alpha_i) (\lambda_i^{\alpha_i} - 1) \quad (6.7)$$

where $i = 1, 2$, and 3 . This equation has six material constants, μ_i and α_i .

The approaches described so far employ a specific form of the equation for relating stress and strain (constitutive equation). The equation contains a number of material constants, which must be determined through fitting the equations to the experimental data. Heretofore, there has been no attempt to relate these material constants to the molecular architecture of gum rubbers.

Next, an approach commonly used for the viscoelastic treatment, which involves non-equilibrium is presented. The following example relates to elongational measurement. Because gum rubber is amorphous, isotropic and incompressible:

$$\lambda_1 = 1 / \lambda_2 \lambda_3 \quad (6.8)$$

and

$$\lambda_2 = \lambda_3 = \sqrt{\lambda_1} \quad (6.9)$$

Therefore, λ_1 is the only independent variable of strain and the elongational stress σ_{11} is a function of λ_1 only:

$$\sigma_{11} = f(\lambda_1) = f'(\varepsilon_1) \quad (6.10)$$

where

$$\lambda_1 = \varepsilon_1 + 1 \quad (6.11)$$

Equation 6.10 may be expressed in terms of tensile modulus with the recognition of time-dependence as

$$E = \sigma/\varepsilon = f''(\dot{\varepsilon}, \varepsilon) \quad (6.12)$$

where $\dot{\varepsilon}$ is the rate of elongation. Also, the subscript is dropped because it is no longer necessary.

When the rate of elongation is constant, time t is given by

$$t = \varepsilon / \dot{\varepsilon} \quad (6.13)$$

and

$$E = f'''(t, \varepsilon) \quad (6.14)$$

The constitutive equation is

$$\sigma = E(t, \varepsilon)\varepsilon \quad (6.15)$$

where the stress and strain are related through the material function $E(t, \varepsilon)$ instead of the material constants. The use of material functions for describing the mechanical behaviour of polymers is the general method in the field of viscoelasticity [6] and this paper follows the convention.

6.3 Non-linear viscoelasticity

When the magnitude of response of a material is proportional to the strength of the imposed field, a linear relationship exists. Typical examples in the field of rheology are Hooke's law:

$$\sigma = E\varepsilon \quad (6.16)$$

and the Newtonian flow equation

$$\tau = \eta \dot{\gamma} \quad (6.17)$$

where τ is the steady state shear stress and $\dot{\gamma}$ is the steady state shear rate. In this case, E and η are material constants.

In the field of viscoelasticity, the definition of linearity is modified to

$$\sigma = E(t)\epsilon \quad (6.18)$$

where $E(t)$ is a function of time, i.e., a material function. The material functions may be the storage modulus $G'(\omega)$ and the loss modulus $G''(\omega)$ of shear dynamic measurements, the relaxation modulus, $G(t)$ and creep compliance $J(t)$. For linear viscoelasticity the material functions are functions of the 'time scale' only. The time scale includes the observed time as well as the frequency ν (Hz) or the angular frequency ω (rad/s). However, the steady state non-Newtonian flow equation

$$\tau = \eta(\dot{\gamma})\dot{\gamma} \quad (6.19)$$

is understood to be non-linear [6].

Gum rubbers in general exhibit linear behaviour at small deformations. For studying mixing of rubber, we must treat large deformations. In this case, modulus is not only a function of time, but also of strain; the relationship is called non-linear. An example with elongational measurements is already stated in Equation 6.15

$$\sigma = E(t, \epsilon)\epsilon$$

When the material behaviour is linearly viscoelastic for a sample (Equation 6.18), $E(t)$ plotted against t forms a curve, which is unique for a given sample; usually a $\log E(t)$ versus $\log t$ plot is used. When the material behaviour is non-linear, as in Equation (6.15), it requires both the t -axis and ϵ -axis to present the sample characteristics as a curved surface.

Where two different samples are concerned, the two curved surfaces must be compared and the process is rather cumbersome. In addition, many measurements are required to construct the characteristic surface.

There have been various attempts to simplify the situation; they are, in general, attempts to 'linearise' the non-linear behaviour. The linearisation is possible in some cases and not

possible in others. In general, it is possible when the ‘separability of time and strain’ holds.

The separability may be explained by the following example

$$E(t, \varepsilon) = F(t)\phi(\varepsilon) \quad (6.20)$$

At the limit, $\varepsilon \rightarrow 0$, it gives $\phi(\varepsilon) \rightarrow 1$ and therefore

$$E(t, \varepsilon \rightarrow 0) = F(t) \quad (6.21)$$

This gives a linear relationship at infinitesimal strain [7]. When equation (6.20) is written as

$$E(t, \varepsilon) / \phi(\varepsilon) = F(t) \quad (6.22)$$

the modulus is linearised through the modification with $\phi(\varepsilon)$. Although these expressions for linearisation, i.e., equations (6.20-6.22), are often cited, the physical meaning of the function $\phi(\varepsilon)$ has not been examined.

The linear behaviour at small deformations may be interpreted as follows. The elongational modulus E is independent of the magnitude of strain, equation (6.16), a fact which means that the internal structure of the material is unaffected by the deformation. Stated the other way around, if the internal structure is altered as a result of the deformation, E must change. Therefore $\phi(\varepsilon)$ is a measure corresponding to the change of the internal structure which is affected by strain ε .

In general, the internal structure is expected to change upon deformation, and non-linear behaviour is the rule at a finite deformation.

However, the gum rubber chain segments, which are shorter than the entanglement coupling distance, are in liquid motion. Therefore, any change in the structure may immediately be relaxed. This may explain the apparent linear behaviour exhibited by many gum rubbers at finite but relatively small deformations.

When rubber crystallises upon stretching, e.g., NR, obviously there is structure change and non-linear behaviour is expected. Even with non-crystallising gum rubbers, non-linear behaviour is observed at large deformations. With the form given in equations (6.20-6.22), the internal structure is affected by strain but is independent of strain rate. The internal structure of rubber is affected by the motion of chain segments and their relaxation times. Therefore, non-linearity should appear in both time-dependence and

strain-dependence. With consideration of both dependences, Schapery gave a general form for the separability of time and strain [8]. His theory is presented [1] for the non-linear creep compliance, $J_u(t)$, and for the non-linear stress relaxation modulus, $G_n(t)$:

$$J_u(t) = \frac{e(t)}{\sigma} = g_0 J_u + g_1 g_2 \Delta J(t / a_\sigma) \quad (6.23)$$

$$G_n(t) = \frac{\sigma(t)}{e} = h_e G_r + h_1 h_2 \Delta G(t / a_e) \quad (6.24)$$

where σ is the stress and e is the strain, J_u is the unrelaxed compliance, i.e., glassy compliance, and

$$\Delta J(t) = J(t) - J_u \quad (6.25)$$

The symbols g_0 , g_1 , g_2 , and a_σ are functions of stress and represent the extent of non-linearity. At the limiting condition, $\sigma \rightarrow 0$, these functions approach one, and represent linearity.

Referring to equation 6.24, G_r is the relaxed modulus, which has a constant value for crosslinked rubber but otherwise is zero:

$$\Delta G(t) = G(t) - G_r \quad (6.26)$$

The symbols h_e , h_1 , h_2 , and a_e are functions of strain and represent the extent of non-linearity. At the limiting condition, $e \rightarrow 0$, all these approach one.

According to the interpretation of this chapter, g_0 , g_1 , g_2 , and h_e , h_1 , h_2 , reflect the changes of internal structure upon application of stress in the former and strain in the latter case, respectively.

The functions a_σ and a_e represent the effect of stress and strain, respectively, on the time scale. This may be explained as follows. When a body is deformed, the corresponding amount of mechanical energy is imparted to the body. This energy brings about a certain degree of excitation. This is analogous to the excitation resulting from thermal energy input. In the latter case, the excitation takes the form of time-temperature correspondence with many polymer melts and rubbers. The extent of temperature effect on time scale is the 'shift' factor', a_T , which is a function of temperature. Likewise, the mechanical excitation is expected to have an influence on time scale [9]. In this case, a_σ and a_e are similar to a_T . The material functions g_0 , g_1 , g_2 , a_σ and h_e , h_1 , h_2 , a_e must be determined

experimentally. Once they are known, linearisation becomes possible for non-linear behaviour.

With many gum rubbers a very simple form of linearisation is possible [10, 11]. In terms of Schapery's theory, it corresponds to $h_e = 0$, $h_1 = 1$, $h_2 = 1$, and $a_e = 1 / \alpha$ for the elongation data:

$$\sigma = E(\alpha)\epsilon \quad (6.27)$$

Because α is the extension ratio, it is a 'universal parameter', which does not require experimental determination.

There are gum rubbers which do not obey the relationship given by equation 6.27. One case is rubber exhibiting strain-hardening. The linearisation in this case is in terms of Schapery's theory, $h_e = 0$, $h_1 = 1$, $h_2 = 1 / \Gamma(\alpha)$, and $a_e = 1 / \alpha$. $\Gamma(\alpha)$ represents the extent of strain-hardening and must be determined from experimental measurements:

$$\sigma = [F(\alpha)\Gamma(\alpha)]\epsilon \quad (6.28)$$

where

$$F(\alpha) = E(\epsilon, t) / \Gamma(\alpha) \quad (6.29)$$

A phenomenological explanation has been given for equations 6.27-6.29 by this author [12] without reference to Schapery's theory. It is a rational analysis of the relationship between macroscopic deformation and the deformation in the segmental level of polymer chains. An increase of free volume resulting from deformation in the dynamic state is the explanation for the strain-time correspondence.

6.4 Conventional methods of characterisation

For a given type of gum rubber, if the compositional aspects such as the comonomer ratio, microstructure and their distributions are known, characterisation becomes centered around the determination of MW, its distribution, and the degree of branching.

For expediency, the DSV (see Chapter 5) is often used as a measure of MW. For the determination of absolute MWs, osmotic pressure measurement is used for number-average and light scattering for weight average. A relative spread of MW distribution is expressed by the ratio of the weight-average to the number-average MW. With the advent of size exclusion chromatography, much more detail of the MW distribution is obtained quickly. The raw data are processed to yield various MW averages, \overline{M}_n , \overline{M}_w , \overline{M}_z , and \overline{M}_{z+1} . For the dilute solution methods of characterisation the theoretical background has been well developed [13]. On the other hand, the information derived from these

methods is often inadequate or even misleading when related to the processability of gum rubbers. There are a number of reasons for this:

- (i) the sample size is so small that it may not be representative of a large commercial lot
- (ii) the solution is so dilute that the response signal may be weak for the part of the information relevant to processability
- (iii) the high MW chains may associate
- (iv) the ultra-high MW fraction may be filtered off
- (v) the gel, i.e., insoluble fraction, is removed by the filters
- (vi) there may be no adequate resolution for the very high MW range
- (vii) there are no calibration standards for the ultrahigh MWs in GPC.

Items (iii), (iv), and (v) give much uncertainty in interpreting results, because of the presence or absence of molecular association, ultra-high MW and gel usually remains unknown. The high MW fraction and gel often have significant effects on processability even though the amount is small.

In production control, GPC data are sometimes collected routinely along with measurements of the Mooney index [14]. When these two sets of data are compared for hundreds of production lots, in only about 50% of cases may a correlation be found. This is partly because the Mooney index is a very crude measure of rubber property, but the uncertainties described above on GPC data are also responsible.

The Mooney index is often called ‘Mooney viscosity’ but there is no rationale that the index represents viscosity. It is an expression of some aspect of viscoelasticity in that there may be some relationship to the processability. The method uses an instrument with a particular design, which provides a simple operation and a quick result. Compared to the dilute solution method, the sample size required is much larger so that it is more representative of the commercial lot. The Mooney index has been used worldwide as a specification for gum rubbers.

However, there is no firm theoretical basis for this index. It is only a very crude method of differentiation between samples; for the same value of the index, the processability of two gum rubbers may be different. In other cases, with rather wide differences in the value of the Mooney index, two rubbers may process almost equally well.

There have been attempts to interpret the meaning of the Mooney index. Often it is assumed that the measurement concerns steady state viscosity at a prescribed temperature.

The standard procedure [14] requires 1 minute of preheating before the rotation is started. Because the temperature is set at for example, 100 °C, the sample is not even in temperature equilibrium. The procedure is obviously a compromise for obtaining the data quickly. The rotational speed being 2 rpm, most of the rubber at 100 °C shows stress-over-shoot (see section 4.3) [6]. The torque value is recorded after 4 minutes of rotation and expressed as the Mooney unit. At 4 minutes, the torque is usually past the peak and in the relaxation part of the curve but not in the steady state. This is shown in Figure 6.1, for somewhat exaggerated examples, which gave the same Mooney index but vary in viscoelastic behaviour.

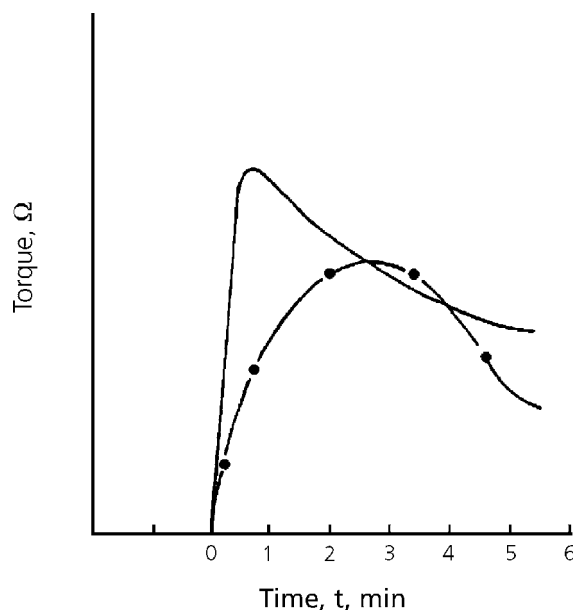


Figure 6.1 Typical Mooney curves; very different viscoelastic properties for the same Mooney indices.

Reprinted from N. Nakajima, Polymer International, 1995, 36, 2, 105. Copyright 1995, SCI. Reproduced with permission.

If sufficient time is given for preheating, more than several minutes, and the rotation is continued, a steady state torque may be observed, [15].

The steady torque is not necessarily the result of the flow, but quite often a result of the fracture of the rubber and the generation of supermolecular flow units [16]. Nevertheless, it is sometimes assumed to be the steady state flow and the steady state viscosity is calculated as a function of shear rate. Such a calculation is quite involved, because of the geometry of

the instrument and non-uniform distribution of shear rates [17]. More useful is the torque rise part of the curve, the transient behaviour from which a complex property may be calculated. Being a complex property, it may be resolved into elastic and viscous contributions. However, 2 rpm is too fast to obtain accurate data of the torque rise. As slow a rate as possible, e.g., 0.05 rpm, is recommended both for reasons of accuracy and for covering a wide range of time scales.

As described in Chapters 4 and 5, an adequate description of gum rubber processability requires a scientific approach; it requires observation of non-linear viscoelasticity and fracture behaviour over a range of temperatures and time. The non-linear viscoelastic data are represented by a curved surface as mentioned earlier in section 6.3 and the fracture behaviour is summarised in a failure envelope. Quite often, numbers (indices) are preferred to graphs and figures for representing a sample; a minimum number of the indices necessary for adequately describing a given gum rubber was determined to be 12, a '12 point characterisation' [18]. If values are known for some of the indices, or if they do not vary among the samples of interest, the number of determinations may be considerably reduced.

The method this author prefers is the use of curves. The surface, representing non-linear viscoelasticity, may be converted to a curve, through the linearisation scheme described in section 6.3. The fracture behaviour is expressed as a failure envelope of the modulus and the strain at break.

6.5 Characterisation based on viscoelasticity

Characterisation of a gum rubber requires determination of the amount of gel fraction, unless it is known to be gel-free. The most direct means of determining gel content is the filtration of the solution. However, the absolute value of gel content is difficult to assess, because the value depends upon the pore size of the filter. Also, the gel is not necessarily distributed uniformly throughout a given lot so that the data are only approximate measures. The viscoelastic method is relative but more reproducible than filtration because the sample size is larger. For a critical examination of the presence of gel, the viscoelastic method provides a better comparison among samples; the filtration results may be used as supplementary information.

The generation of a macrogel, a highly branched insoluble molecule, begins with the formation of long branches. At present, there is no clear knowledge about how many long branches per molecule must form before it becomes insoluble. Because our present interest is in processability and not in solubility, long branches and gel may be considered to be of the same kind but differing in degree. The following method may be used for evaluating the relative degree of long branching or gel content. Firstly, shear dynamic measurements are performed to obtain storage modulus $G'(\omega)$ and loss modulus $G''(\omega)$. Then, G' and G'' are

taken at the same value of ω , and plotted as $\log G''$ versus $\log G'$. Examples are shown in Figure 6.2 for the samples of NBR which are listed in Table 6.1 [19].

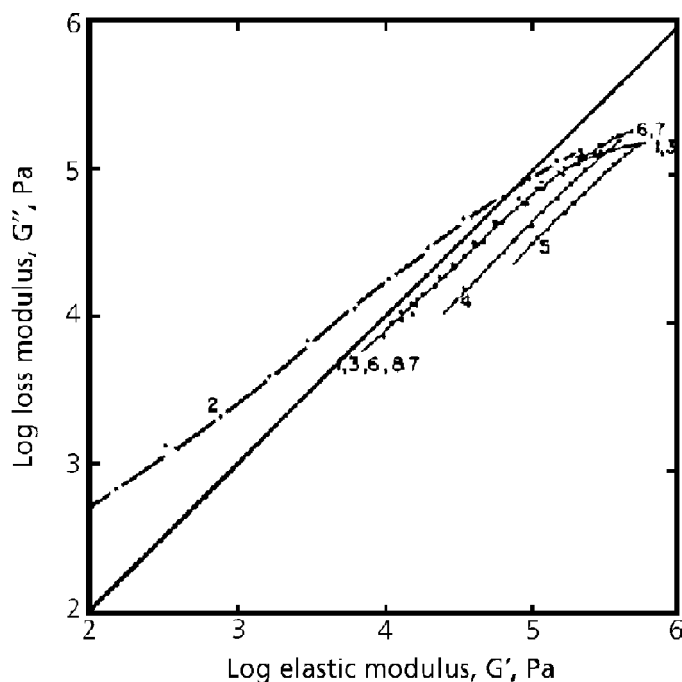


Figure 6.2 Log G'' - log G' curves of NBR samples 1-7 (see Table 6.1).

Reprinted from N. Nakajima, *Polymer International*, 1995, 36, 2, 105. Copyright 1995, SCI. Reproduced with permission.

Table 6.1. Characteristics of butadiene-acrylonitrile copolymer samples			
Sample	Mooney ^b index ML-4-100	Acrylonitrile content of polymer (%)	Gel ^a (%)
1	71	43.7	0.9
2	22	41.2	0.1
3	121	39.4	0.1
4	103	40.3	54.7
5	88	40.9	71.7
6	52	33.8	0
7	56	28.4	5.11

^aASTM D 3616-95 [20], only an approximate measure
^bASTM D 1646-96a [14]

Samples 1, 6, and 7 are so-called 'gel-free', commercial polymers, containing acrylonitrile of 44, 34, and 28%, respectively. The gel determination is based on ASTM D 3616-95 [20], which requires a screen having a 300 μm opening. If a GPC filter with 0.1 ~ 0.2 μm opening is used, a significant amount of gel may be found in the 'gel-free' polymer. The ASTM test is intended to give a pragmatic definition of gel content in such a way that if a sample is gel-free according to this analysis, the effect of gel on the processability is negligible. Strictly speaking, the above statement may not be acceptable in some cases. Therefore, for each polymer type and for each processability requirement, the assumptions involved in the gel determination need to be examined.

Returning to Samples 1, 6, and 7, the $\log G''$ versus $\log G'$ curves of these polymers are the same; this fact indicates that these polymers have the same degree of long branching and are 'gel-free'.

Next, Samples 1, 2, and 3 are compared. Samples 2 and 3 were made in a pilot plant under the same polymerisation conditions (except for MW) as that of the commercial product, Sample 1. Sample 2 is made to a lower MW with the use of a modifier, which also suppresses the long branch formation. Sample 3 is made to have a higher MW. Samples 4 and 5 contain significant amounts of gel.

In Figure 6.2, the curves of the seven samples form four groups. Sample 2 containing the least long branches lies on the left; the 'gel-free' samples, 1, 3, 6 and 7, are in the middle; Sample 4 containing 55% gel is on the right; and Sample 5 containing 70% gel is on the far right. This figure illustrates that from the position of $\log G''$ versus $\log G'$ plots, the degree of long branching or the gel content may be assessed.

The 45° line in the figure represents $G'' = G'$. The curve of Sample 2 is above this line, $G'' > G'$. The data of this sample are in the flow region. The curves of all other samples are in the state $G' > G''$, indicating the dominance of elastic behaviour over viscous behaviour. In the earlier chapters, the mill processability of gum rubber was interpreted on the basis of whether elasticity or viscous loss dominates. Although the mill processability involves large deformation and the data of Figure 6.2 are limited to small deformations, an approximate relationship between Figure 6.2 and the mill processability may be found. Only one exception to this relationship, but a very important one, is gum rubber containing microgel. The microgel is a particle containing a crosslinked network, which may be formed during emulsion polymerisation with difunctional co-monomer [21]. The response of microgel to processability is entirely different from that of macrogel, and yet in Figure 6.2 only gel content may be assessed but not the difference between macrogel and microgel.

In order to differentiate between gel types, large deformation measurements must be performed and the strain-time correspondence must be used for linearisation. The elongation measurements performed at a constant temperature and various elongation rates are expressed

as the elongational modulus $E(\alpha t)$. With some gum rubbers, $E(\alpha t)$ becomes a master curve, which is independent of the elongation rates, and with others it is rate dependent. The former type is either gel-free or contains a small amount of macrogel and any amount of microgel. The latter type shows strain-hardening and contains a significant amount of macrogel. Typical examples are shown in Chapter 4, but additional examples are now given.

Instead of using elongational modulus, the equivalent of complex viscosity may be used:

$$\eta_T = E(\alpha t)\alpha t \quad (6.30)$$

In this case, η_T is expressed as a function of the reduced rate, $1/\alpha t$. If linearisation holds, $1/\alpha t$ is numerically equal to ω . Further, for a Poisson's ratio of 0.5, η_T is related to shear complex viscosity $|\eta^*|$ as

$$\eta_T = 3 |\eta^*| \quad (6.31)$$

In this manner large deformation elongational data may be compared with small deformation shear data. A number of examples are presented below in the form of equation (6.31).

Figure 6.3 shows the data for sample C of NBR with 33% acrylonitrile containing about 50% of microgel.

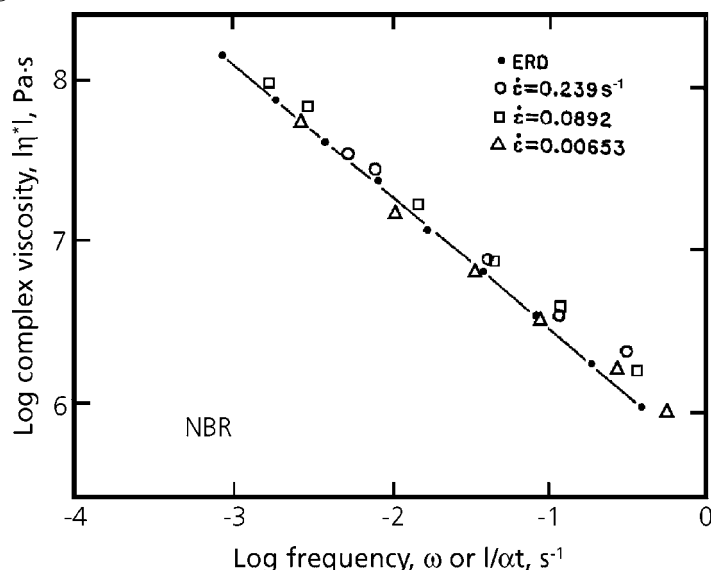


Figure 6.3 Comparison of viscosities calculated from tensile measurements with dynamic shear viscosities for sample C of NBR with 33% acrylonitrile and about 50% microgel. Shear viscosities, ERD; elongation rate, $\dot{\epsilon}$.

Reprinted from N. Nakajima, *Polymer International*, 1995, 36, 2, 105. Copyright 1995, SCI. Reproduced with permission.

There is some scatter in data points but the data at three different elongation rates form a master curve, which is also in agreement with the shear data as per equation (6.31). Figures 6.4 and 6.5 are for a sample of SBR 1502, and a sample of SBR 1712, respectively, both being gel-free. SBR 1712 is an oil-extended gum rubber. A sample of polyisobutylene is shown in Figure 6.6. All three samples, even though chemical compositions are quite different, obey the strain-time correspondence. The elongational and the shear data are in good agreement, equation (6.31).

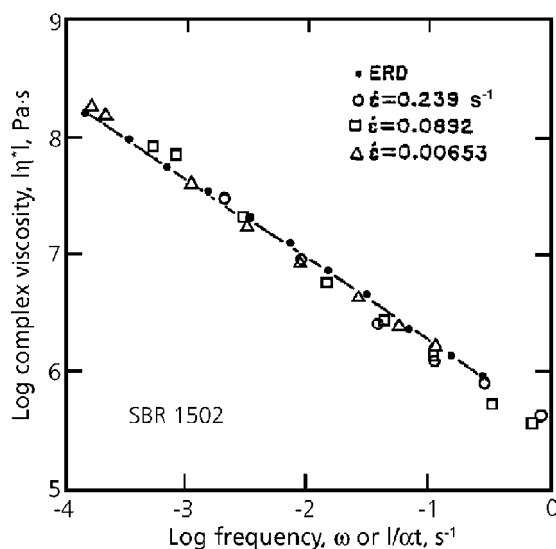


Figure 6.4 Comparison of viscosities calculated from tensile measurements with dynamic shear viscosities for a sample of SBR 1502. Shear viscosity, ERD; elongation rate, $\dot{\epsilon}$.

Reprinted from N. Nakajima, *Polymer International*, 1995, 36, 2, 105. Copyright 1995, SCI. Reproduced with permission.

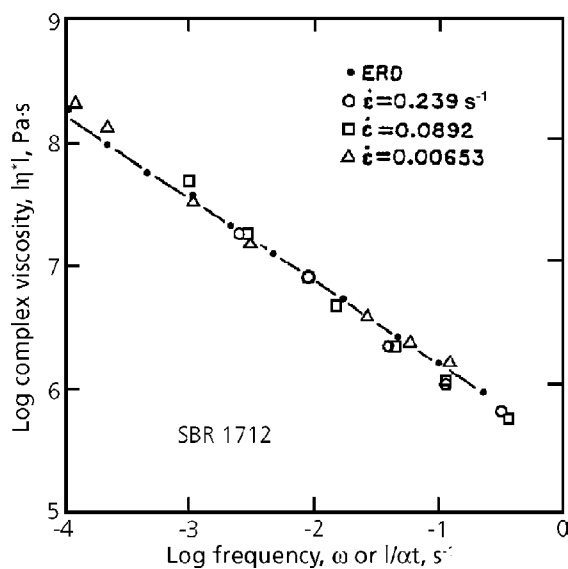


Figure 6.5 Comparison of viscosities calculated from tensile measurements with dynamic shear viscosities for a sample of SBR 1712. Shear viscosity, ERD; elongation rate, $\dot{\epsilon}$.

Reprinted from N. Nakajima, *Polymer International*, 1995, 36, 2, 105. Copyright 1995, SCl. Reproduced with permission.

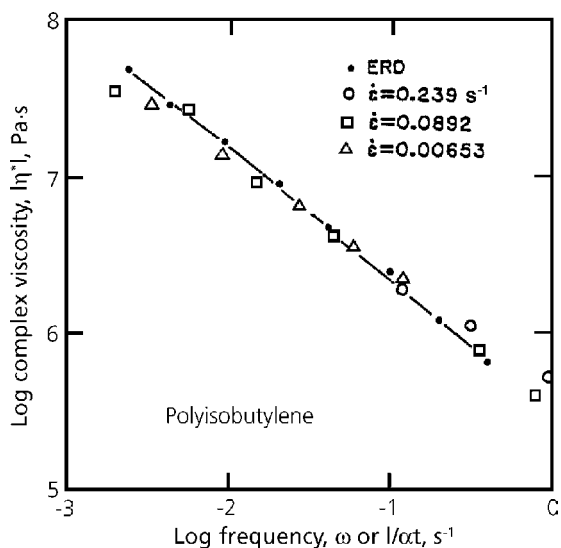


Figure 6.6 Comparison of viscosities calculated from tensile measurements with dynamic shear viscosities for a sample of polyisobutylene. Shear viscosity, eccentric rotating disk (ERD); elongation rate, $\dot{\epsilon}$.

Reprinted from N. Nakajima, *Polymer International*, 1995, 36, 2, 105. Copyright 1995, SCl. Reproduced with permission.

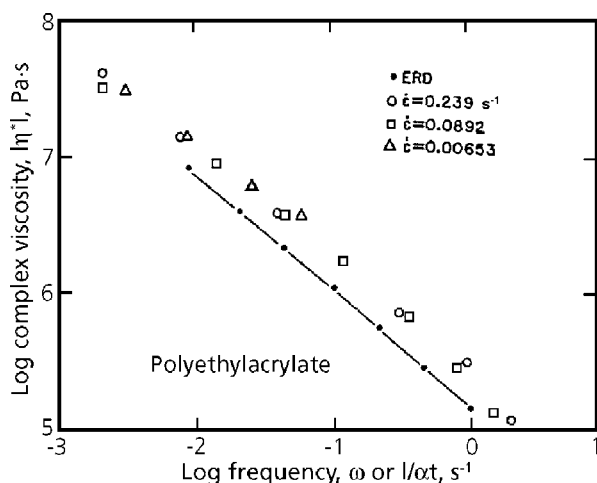


Figure 6.7 Comparison of viscosities calculated from tensile measurements with dynamic shear viscosities for a sample of polyethylacrylate. Shear viscosity, ERO; elongation rate, $\dot{\epsilon}$.

Reprinted from N. Nakajima, *Polymer International*, 1995, 36, 2, 105. Copyright 1995, SCI. Reproduced with permission.

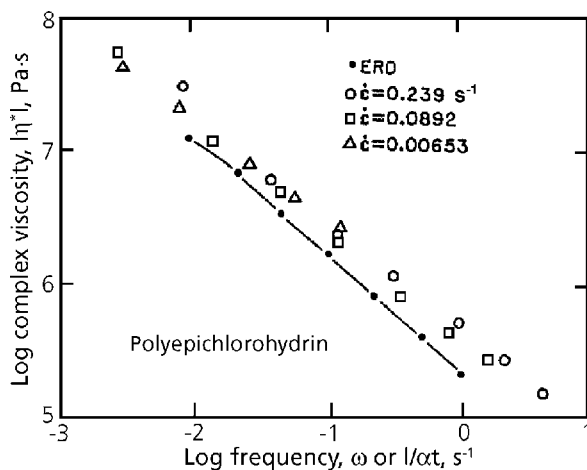


Figure 6.8 Comparison of viscosities calculated from tensile measurements with dynamic shear viscosities for a sample of polyepichlorohydrin. Shear viscosity, ERO; elongation rate, $\dot{\epsilon}$.

Reprinted from N. Nakajima, *Polymer International*, 1995, 36, 2, 105. Copyright 1995, SCI. Reproduced with permission.

Examples of polyethylacrylate and polyepichlorohydrin, are shown in Figures 6.7 and 6.8, respectively.

These polymers consist of polar monomeric units. They are very different from diene rubbers and polyisobutylene. The elongational data of these polymers obey the strain-time correspondence and form master curves. But the elongational and shear data do not agree:

$$\eta_T > 3 |\eta^*| \quad (6.32)$$

This behaviour may be attributable to intermolecular polar association, which may be weak at small deformations but becomes significant at large deformations, somewhat analogous to strain-induced crystallisation. With NBR having a high polar content, i.e., above 40% acrylonitrile, a similar observation was made about polar association [22]. One note of caution is the effect of humidity on the viscoelastic properties of rubber containing polar groups [23]. The absorbed moisture may prevent the polar association. This can happen in humid climates or when the gum rubber is not completely dried. This aspect warrants further investigation.

Gum rubber is not a crosslinked network, but for some reason if a network is formed, the elongational data are as shown in Figure 6.9.

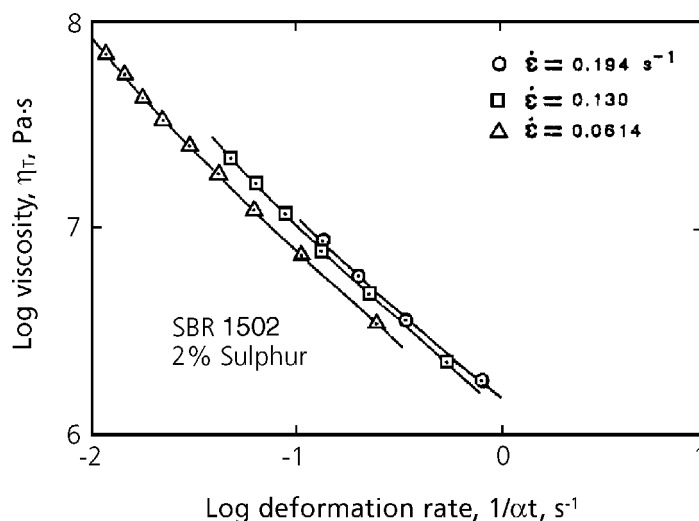


Figure 6.9 Application of strain-line correspondence principle to the tensile stress-strain data of SBR 1502 crosslinked with 2 phr of sulphur.

Reprinted from N. Nakajima, *Polymer International*, 1995, 36, 2, 105. Copyright 1995, SCI. As Figure 6.1.

The data at different elongation rates do not obey strain-time correspondence but form different curves, which have an upturn indicating limited extensibility [22].

Some gum rubbers obey strain-time correspondence. Other rubbers do not obey the principle, because of strain-hardening. There is yet another type which does not obey strain-time correspondence, because it exhibits linear behaviour even at rather large deformations. In general this type of rubber is soft, and it may be difficult to obtain accurate elongational data. By using a rotational rheometer operated at very low speeds in order to avoid slip, it is possible to obtain accurate data at large shear strains [24].

For shear stress τ and shear strain γ the shear modulus G is

$$G = \tau/\gamma \quad (6.33)$$

Because shear strain rate $\dot{\gamma}$ is constant, the time t is

$$t = \gamma/\dot{\gamma} \quad (6.34)$$

For linear behaviour, viscosity η is

$$\eta = \tau/\dot{\gamma} = G t \quad (6.35)$$

and at equal values of ω and $1/t$

$$\eta = |\eta^*| \quad (6.36)$$

the viscosity η has an equal value to that of the complex viscosity.

For non-linear behaviour which obeys strain-time correspondence, viscosities η and $|\eta^*|$ are equal at equal values of ω and $1/\alpha t$. Instead of equation (6.35), viscosity has the form

$$\eta = G \alpha t \quad (6.37)$$

or

$$\eta = (\tau/\dot{\gamma})\alpha = |\eta^*| \quad (6.38)$$

The relationship between shear strain and the extension ratio is given as [15]:

$$\gamma = \alpha - (1/\alpha) \quad (6.39)$$

An example with an ethylene-propylene rubber of Mooney index 40, is shown in Figures 6.10a and 6.10b.

The points in the figures represent η and the lines $|\eta^*|$. Figure 6.10a shows that the linear form, equation (6.35), holds, and Figure 6.10b shows that the non-linear, strain-time correspondence, equation (6.37), does not hold.

On the other hand, an NBR with a Mooney index of 35 and acrylonitrile content of 33% does not obey equation (6.35), see Figure 6.11a, but obeys the non-linear equation (6.37), see Figure 6.11b.

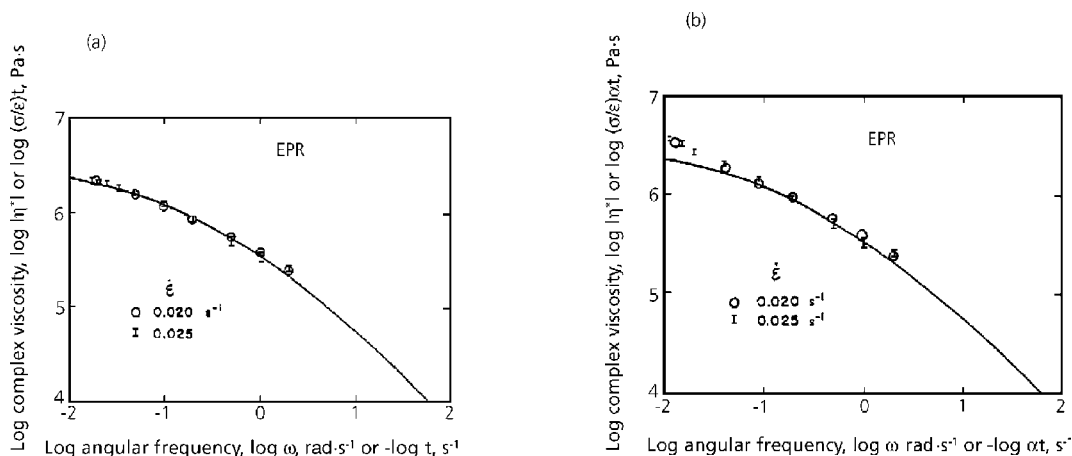


Figure 6.10 (a) Complex viscosity of ethylene-propylene rubber (EPR) at 30 °C. The line represents the observed data and the markings are the data calculated from the stress rise at a constant deformation rate. The calculation is based on linear viscoelasticity. The stress rise measurements at $\dot{\epsilon} = 0.025 \text{ s}^{-1}$ were performed in triplicate. The figure shows agreement between calculated and observed data. (b) The same data as in (a), except that the calculation is based on the non-linear relation, the strain-time correspondence.

This figure shows disagreement between calculated and observed data.

Reprinted from N. Nakajima, Polymer International, 1995, 36, 2, 105. Copyright 1995, SCI. Reproduced with permission.

The rubber exhibiting linear behaviour, Figure 6.10a, tends to go to the flow state where viscous contribution dominates over the elastic contribution. This type of rubber has a relatively low MW and no significant long branching. On the other hand, a rubber exhibiting non-linear behaviour, Figure 6.11b may have a high MW, some long branching, and even a small amount of macrogel. The Mooney values of these two rubbers are very similar, but the viscoelastic behaviour of these rubbers is very different.

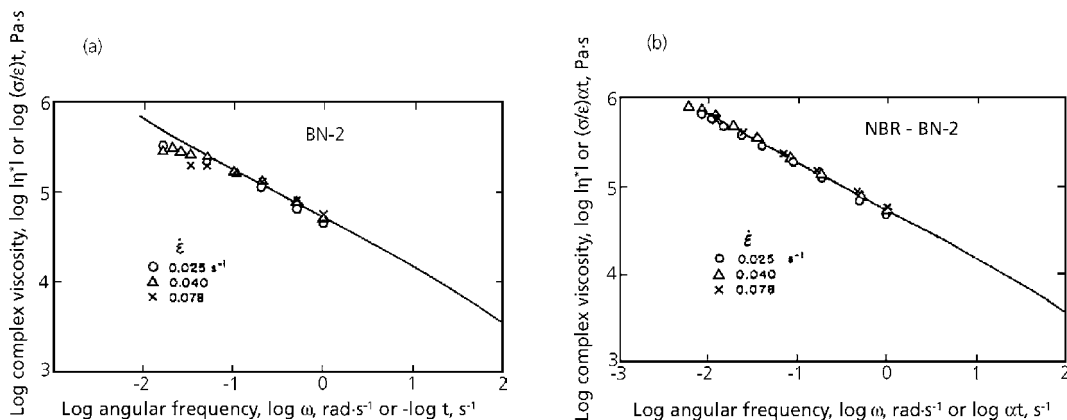


Figure 6.11(a) Complex viscosity of NBR sample BN-2 at 100 °C. The line represents the observed data and the markings are the data calculated from the stress rise at constant deformation rates. Three different rates were used. The calculation is based on linear viscoelasticity. This figure shows disagreement between calculated and observed data. (b) The same data as in (a), except that the calculation is based on the non-linear expression, the strain-time correspondence. This figure shows agreement between calculated and observed data.

Reprinted from N. Nakajima, Polymer International, 1995, 36, 2, 105. Copyright 1995, SCI. Reproduced with permission.

As stated before, the presence or absence of gel is the first and a most important aspect of gum rubber characterisation. When gel is present, the concept of MW loses practical meaning, because the MW of gel is extremely high and cannot be measured. Nevertheless, when two gum rubbers are compared, the question may arise as to which has the higher MW. In such a case, because the comparison of MWs has no real meaning, the question may be redirected to the level of the viscoelastic properties.

The Mooney index is usually used for this comparison. However, this practice may be misleading because in some cases, a higher gel content gives a lower Mooney index [21]. What is needed here is some measure of viscoelastic property, which gives a higher value for a higher gel content. If gel is absent, the same property should give a higher value for a higher MW. For this purpose the dynamic complex viscosity at low frequencies may be used. Figure 6.12 shows gel-free EPM. At low frequencies, samples of a higher weight-average MW \overline{M}_w have a higher $|\eta^*|$ [25].

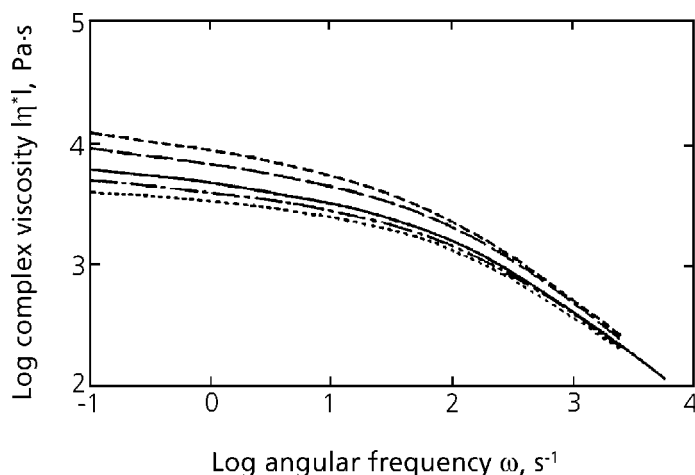


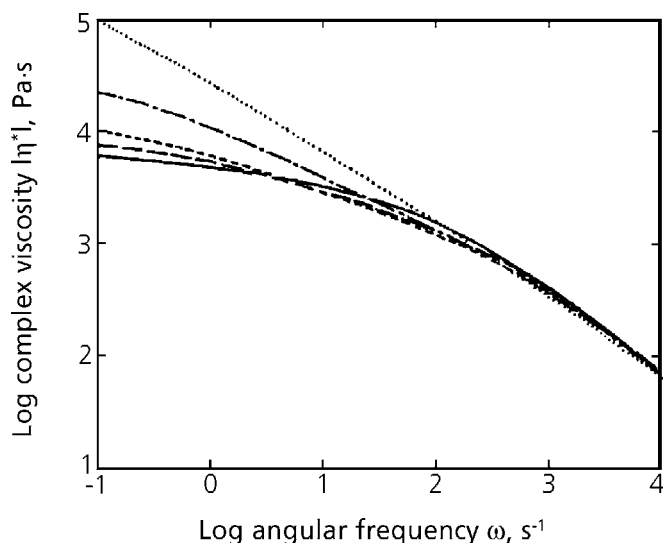
Figure 6.12 Effect of variation in \overline{M}_w on the complex viscosity curves at 230°C: (.....) A, 1.13×10^5 ; (— · —) B, 1.35×10^5 ; (— —) C, 1.56×10^5 ; (— · —) D, 1.70×10^5 ; (—) XL-0, 1.16×10^5 .

Reprinted from N. Nakajima, *Polymer International*, 1995, 36, 2, 105. Copyright 1995, SCI. Reproduced with permission.

When the EPM is milled in presence of a peroxide, long branches and gel are generated. As shown in Table 6.2 the different amounts of peroxide do not give a systematic relationship with GPC data nor with DSV.

Table 6.2. GPC measurements of EPMS with differing amounts of long branches ^a							
Sample Designation	Dicumyl Peroxide (phr)	(10 ⁴)	(10 ⁵)	(10 ⁵)		(10 ⁵)	DSV ^b
XL-0	0.0	5.37	1.16	2.87	2.16	1.04	1.45
XL-1	0.05	4.96	1.04	2.31	2.10	0.94	1.40
XL-2	0.1	4.34	0.96	2.34	2.22	0.86	1.33
XL-3	0.2	4.52	1.18	4.33	2.61	1.02	1.38
XL-4	0.4	4.53	2.37	41.57	5.23	1.64	1.67
^a Symbols \overline{M}_n , \overline{M}_w , \overline{M}_z , describe relative hydrodynamic size, i.e., MW averages are not corrected for branching ^b DSV determined with a concentration of 0.1 g/ml in toluene at 25 °C \overline{M}_v : viscosity average MW							

Unknown amounts of gel must have been removed by filtration. On the other hand, $|\eta^*|$ values at low frequencies in Figure 6.13 are higher for larger amounts of peroxide, clearly indicating the generation of more long branches and gel.



6.13 Effect of increasing long branching (XL-0 - XL-4) on the complex viscosity master curves at 230 °C: (—) XL-0; (— —) XL-1; (---) XL-2; (-. -) XL-3; (.....) XL-4.

Reprinted from N. Nakajima, Polymer International, 1995, 36, 2, 105. Copyright 1995, SCI. Reproduced with permission.

A summary of the viscoelastic characteristics of gum rubber is given below.

1. Relative but quantitative method for the degree of long branching and gel content. Preparation of $\log G''$ versus $\log G'$ plot. For a higher degree of long branching and higher gel content the curve is placed to the right. With reference to the line $G'' = G'$, the position of the curve shows whether viscous behaviour or elastic behaviour dominates.
2. Differentiating macrogel and microgel. Perform elongation measurements with different rates of elongation and test the applicability of strain-time correspondence. Those rubbers obeying the principle are either linear molecules, molecules with long branching but gel-free (ASTM D3616-95) [20], those containing microgel, or in some cases containing a small amount (<10%) of macrogel. Those containing macrogel, e.g., more than approximately 10%, tend to give strain-hardening.

Linearisation requires shifts in both time axis by α and modulus axis by $\Gamma(\alpha)$. The latter represents a relative degree of macrogel content.

3. Rubbers exhibiting linear viscoelastic behaviour. These have either a low MW, a linear molecule, a few long branches, or all of these. The MW distribution is narrow in the sense that there is no excessive spread towards high MWs. Of course, they are gel-free.
4. Differentiating macrogel from microgel when the former is less than 10%. Compare the elongational data with the shear data according to the method given earlier equation (6.27), i.e., without applying the modulus shift. In the presence of macrogel, the elongational modulus divided by a factor of three is higher than the shear modulus.
5. In method 4, there is a case where shear modulus is higher than the elongational modulus (after dividing by three). Examples are triblock copolymers; in small strain shear measurements the physical crosslinks remain intact, but in large strain elongational measurements the crosslinks are destroyed, thus softening the rubber [26].
6. With rubbers having many polar groups, e.g., polyethylacrylate, polyepichlorohydrin, and NBR with 40% acrylonitrile, elongational modulus (divided by three) is higher than shear modulus even in the absence of macrogel. A molecular association similar to strain-induced crystallisation appears to occur at high elongation.
7. In the presence of absorbed moisture, the molecular association may not occur.
8. Complex viscosity at low frequency is a good measure of the 'MW' of a rubber regardless of the presence or absence of gel.

6.6 Processability and molecular structure

Certain specific samples of gum rubber are said to have a good processability or poor processability. These statements have no real meaning unless the processing conditions are specified. For example, the presence of long branching may improve processability or harm it. Therefore, a generalised relationship does not exist between processability and molecular structure. With a full understanding of this difficulty, a discussion is given here on the subject; however, the relationships given are not without exceptions.

During the Second World War, in the early days of the emulsion polymerisation of synthetic rubbers, macrogels were generated which caused difficulty in the milling process. If the

polymerisation temperature was too high, 'hot rubber' was produced. The 'cold rubber' process was developed later, producing easy processing rubber. Macrogel is also produced at high conversion; therefore, the degree of conversion (of monomer to polymer) is limited to a certain percentage. Even with 'gel-free' rubber according to ASTM D3616-95 [20] gel may be detected by the use of a GPC filter. The implication is that below a certain size, or at less than a certain gel content, the macrogel has no adverse effect on mill processability.

In some cases the presence of macrogel is preferred. When a large amount of reinforcing filler must be compounded, the compound tends to become crumbly and breaks into pieces, i.e., 'dry'. In this case, dispersion of carbon black is not achieved and the compound cannot be formed into a shape. The presence of large amounts of macrogel can overcome this problem.

Macrogel-containing rubber may be oil-extended to alleviate the milling problem. Sometimes oil-extended rubber has a superior strength as a vulcanisate compared with the gel-free, non-oil-extended counterpart.

Without oil extension, macrogel-containing rubber has a low tensile strength as a vulcanisate compared with gel-free rubber. This is because branch points increase the crosslink density, thereby limiting the elongation to break.

When green strength is needed for the mixed compound, long branches and even, to some extent, the presence of gel are appreciated. The green strength is the resistance to drape of the sheet made of the uncrosslinked compound.

The presence of long branches and gel generates more free ends in vulcanisates compared with linear molecules. Such free ends increase heat build-up of finished products under repeated stressing.

Mill processability also depends upon the additives in the formulation. Oils, plasticisers and even small amounts of powder [27] affect the mill performance. However, the present discussion will be confined to gum rubbers only.

The most significant difference is found among different types of rubber; *cis*-1,4-polybutadienes being polymerised in solution, the MW distribution is less spread out at the high MW end compared with emulsion polymerised SBR. For this reason and because of the low T_g , some grades of this rubber may tend to go into Region III of mill processability [28] causing mixing problems. The presence of long branches imparts long relaxation times (see section 6.8) and the mixing problem may be overcome. More discussion of this will be given in section 6.7.1.

Even with emulsion polymerisation, polyethylacrylate rubber tends to go into Region IV of mill processability, i.e., the flow region. This is because the rubber has 73% of its MW as the pendent group. It is a fat and short molecule compared with diene rubber. The presence of some long branches may help mill processability. However, when the tendency for Region IV behaviour is known, upside-down mixing, i.e., charging carbon black first into an internal mixer and then the rubber, is the usual practice.

Microgel is a crosslinked latex particle. Rubber containing a large amount of microgel breaks down easily on milling, hence decreasing time and energy of mixing [29]. However, the strength of vulcanisate is somewhat inferior because it gives a lower elongation to break. The microgel-containing compounds tend to give a smoother extrudate. Extrudate swelling is reduced and the degree of swelling is independent of the extrusion rate. The spread of MW distribution towards lower MW has no detrimental effect on processability. The mechanical strength is decreased and the heat build-up is increased in the finished product.

Although much knowledge has been systematically accumulated on the linear viscoelastic behaviour of gum rubber, attempts to relate the linear behaviour to processability may result in misleading or even wrong conclusions. Gum rubber processing involves non-linear behaviour and fracture, which may not be predictable from linear behaviour.

6.7 Processability and viscoelastic characteristics

6.7.1 *Cis*-1,4-polybutadiene

Bearing the cost-benefit relationship in mind, an important question is what is the minimum activity required for obtaining sufficient information on the characteristics of a given gum rubber. Section 6.6 showed that at least two types of measurement are required; one is the dynamic mechanical measurements over the temperature and the frequency region covering processing conditions. The other is the tensile stress-strain measurements at room temperature with at least three and preferably four strain rates. In this section examples are presented to show how this characterisation scheme is used to determine structure-processability relationships.

The first example uses *cis*-1,4-BR. A major application of *cis*-1,4-BR is for tyres. The rubber improves wear resistance, rolling resistance, and flexibility at low temperature. It is usually blended with other rubbers, such as NR or SBR because it does not have a good processability, flex-crack resistance and green strength. Because the rubber has a very low T_g of $-112\text{ }^{\circ}\text{C}$, it tends to fall in Region III or IV of the mill processability.

In order to overcome the problems associated with milling, long branching is considered to be one of the variables to manipulate. Questions are how much and how long the long

branch should be. In addition *cis*-1,4-BR is known to give a strain-induced crystallisation under favourable conditions. Does the strain-induced crystallisation occur during mill-mixing and if so, what effect does it have? Another question is the effect of addition of crystalline particles on the mill processability and strain-induced crystallisation.

The mechanism of branch formation is discussed in Section 1.1.3. In the free radical polymerisation, the chain-transfer mechanism is responsible and the branched molecule becomes more branched leading to gel-formation. In the metal-coordinated catalyst systems used for *cis*-1,4-BR polymerisation, branches are formed by insertion of macromers. Once insertion occurs, the probability of another insertion is considerably decreased because of the steric effect. Therefore, no gel is formed. Not only are fewer branches present but also the branch pattern is different from those in the free-radical polymerised rubbers.

- *Experiment - I* [30]
- *Samples*

The samples were four commercial polybutadienes produced by Bayer AG, see Table 6.3.

Table 6.3 Properties of <i>cis</i> -1,4-butadiene samples ^a				
Sample	BUNA CB11 ^b	BUNA CB22 ^b	BUNA CB23 ^b	BUNA CB24 ^b
Catalyst	Ti	Nd	Nd	Nd
<i>Cis</i> -1,4-(%)	93	98	98	98
1,2-vinyl (%)	4	1	1	1
$\bar{M}_w \times 10^{-4}$ ^c	51	53	51.5	66.5
$\bar{M}_n \times 10^{-4}$ ^c	12	20.5	15	12
\bar{M}_w/\bar{M}_n ^c	4.3	2.6	3.4	5.5
MV ^d	47	63	51	44
T _g (°C)	-105	-109	-109	-109
Degree of branching (%) ^e	10	5	5	3
a: All data supplied by the manufacturer b: Registered Trade mark of Bayer AG c: Data obtained by GPC; MW are not absolute but relative values based on the hydrodynamically equivalent volume of polystyrene standards d: Mooney Index e: Calibrated with star-branched polymers \bar{M}_w : mass-average MW \bar{M}_n : number-average MW MV: Mooney Viscosity				

The sheets of gum rubbers were prepared by pressing at 140 °C for 10 minutes. After removal from the press, the sheets were cut in quarters, piled in four layers, and pressed again under the same conditions to completely remove bubbles. After the second pressing the sheets were placed between two steel plates at room temperature with heavy weights placed on top. The sheets were allowed to rest at least 2 days under the heavy weights to prevent wrinkling when removed.

Oscillatory shear specimens were cut from the sheets as discs 25 mm in diameter and tensile specimens were cut using the dumbbell die C described in ASTM D412 [31].

The gel contents of the sheets were measured by dissolving about 0.4 g of rubber in 100 ml of *n*-heptane for 48 h. The solution was filtered through a Whatman No. 4 filter paper. The filter paper was weighed before and after filtration to estimate the amount of gel removed from the solution. The filtered solution was evaporated in an oven at 110 °C and the amount of dissolved polymer was measured. No gel was found in these samples.

- *Instruments*

The oscillatory shear measurements were performed with a Rheometrics mechanical spectrometer (RMS 800) with parallel plates. The angular frequency range was from 10^{-2} to 10^2 rad/s. The samples were tested at 30, 60, 120, and 150 °C. In addition to the calibration specified by the instrument manufacturer, a standard silicone rubber (SE30; General Electric Company) was used every time to double-check the calibration. The frequency sweep was made from the lowest to the highest and then reversed to the lowest frequency. The data at the lowest frequency should be reproducible if there is no degradation during the measurements.

Tensile tests were performed with a Monsanto Tensometer 500. The strip chart recorder recorded force against time. The force was measured with a 0.45 kg load cell. The extent of deformation was measured by recording with a video camera. An extensometer was not used because the samples were not strong enough to hold it. The samples were held with plastic grips having relatively loose springs in order to prevent breaking at the grips. The tests were performed at room temperature with strain rates of 0.004, 0.017, 0.057, 0.118, and 0.250 s^{-1} .

- *Results and discussion*

- *Oscillatory shear measurements*

Time-temperature superposition was performed in the following sequence: first, $\tan \delta$ data were plotted against $\log \omega$. The superposition involves the $\log \omega$ axis only, because any modulus-shift in G' and G'' cancels out. From this procedure the time-shift factor, a_T , was evaluated. Next, $\log |G^*|$ data were plotted against $\log \omega a_T$. From these plots

the modulus-shift factor, β_T , was evaluated. The results of superposition are shown in Figures 6.14-6.17, where all the data were reduced to 30 °C.

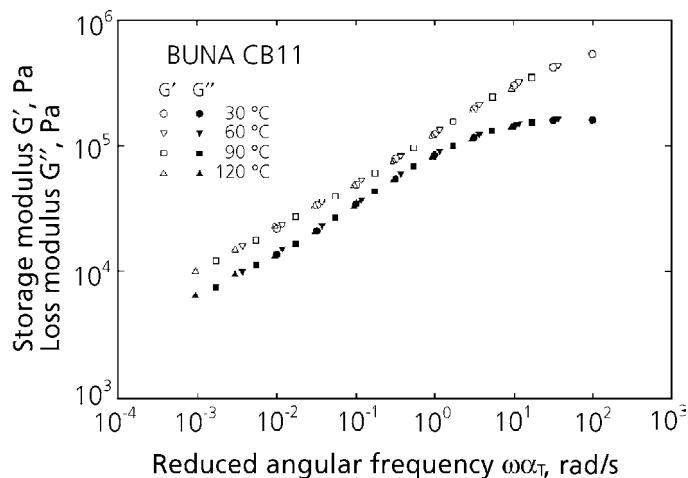


Figure 6.14 Master curves of storage and loss modulus of Buna CB11 (Reference temperature 30 °C).

Reprinted from N. Nakajima and Y. Yamaguchi, *Journal of Applied Polymer Science*, 1996, 61, 9, 1525. Copyright 1996, reprinted by permission of John Wiley and Sons, Inc.

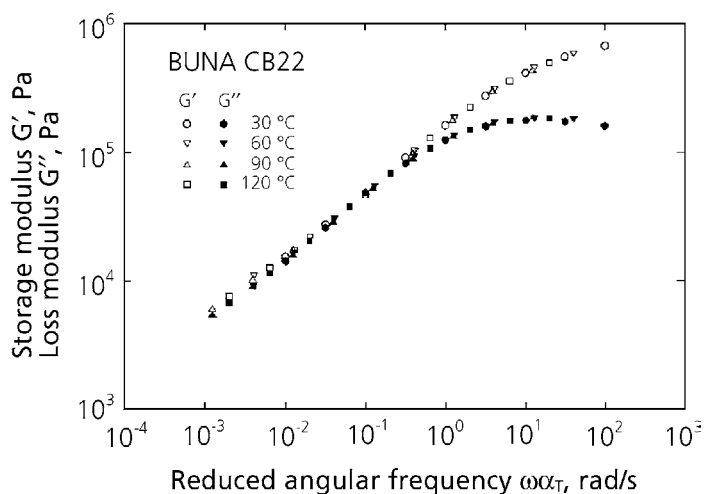


Figure 6.15 Master curves of storage and loss modulus of Buna CB22 (Reference temperature 30 °C).

Reprinted from N. Nakajima and Y. Yamaguchi, *Journal of Applied Polymer Science*, 1996, 61, 9, 1525. Copyright 1996, reprinted by permission of John Wiley and Sons, Inc.

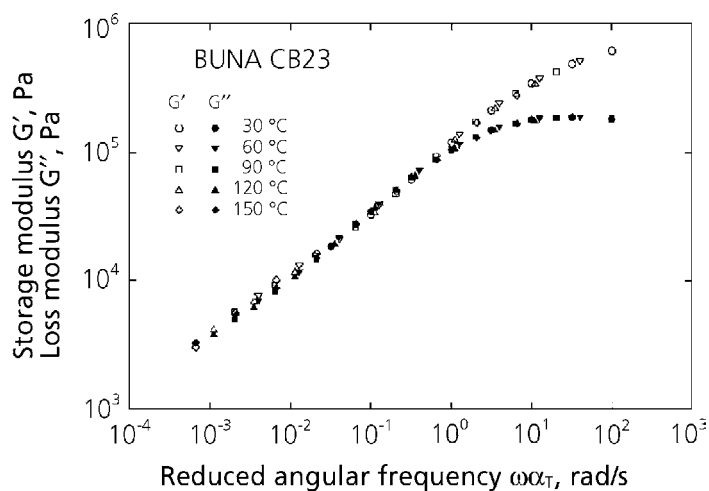


Figure 6.16 Master curves of storage and loss modulus of Buna CB23 (Reference temperature 30 °C).

Reprinted from N. Nakajima and Y. Yamaguchi, *Journal of Applied Polymer Science*, 1996, 61, 9, 1525. Copyright 1996, reprinted by permission of John Wiley and Sons, Inc.

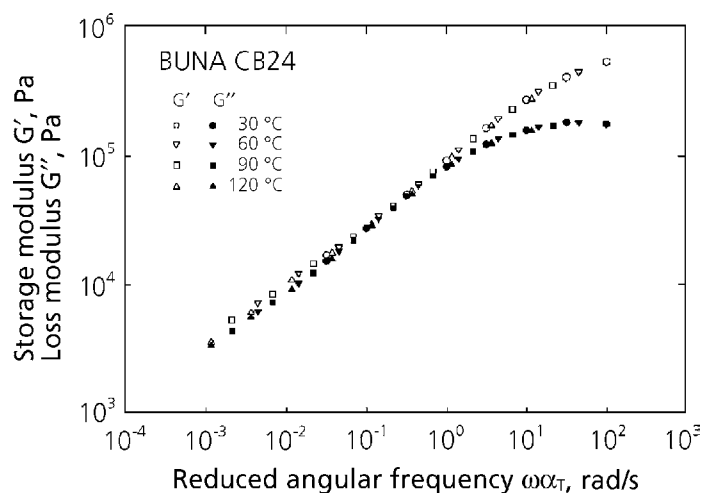


Figure 6.17 Master curves of storage and loss modulus of Buna CB24 (Reference temperature 30 °C).

Reprinted from N. Nakajima and Y. Yamaguchi, *Journal of Applied Polymer Science*, 1996, 61, 9, 1525. Copyright 1996, reprinted by permission of John Wiley and Sons, Inc.

The extent of time-shift was rather small; for the data obtained at 30-120 °C, the frequency range was extended only about one decade to lower frequencies. This is because the glass-transition temperature of *cis*-1,4-BR is very low, -110 °C. All master curves approach the plateau region at the higher frequencies. The lower frequency region is the transition from the plateau towards terminal region. However, these curves do not show a crossover of G' and G'' . They are almost parallel to each other. This indicates that all these samples have some branching. In Figure 6.18, G' curves of four samples are compared.

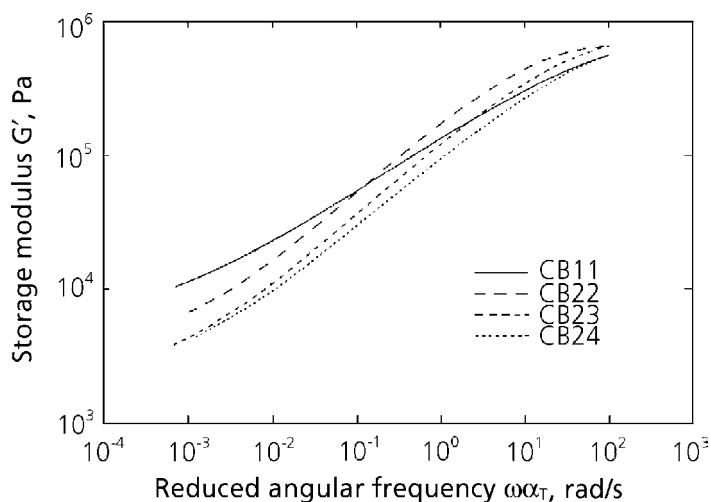


Figure 6.18 Compression of master curves of storage modulus of various Buna samples. (Reference temperature 30 °C).

Reprinted from N. Nakajima and Y. Yamaguchi, *Journal of Applied Polymer Science*, 1996, 61, 9, 1525. Copyright 1996, reprinted by permission of John Wiley and Sons, Inc.

The curve of CB11 shows a smaller slope and higher G' than those of the other samples at low frequencies. This indicates that CB11 contains a structure having a longer relaxation time compared, for example, to CB24. This cannot be explained from the differences in MW and its distribution because CB24 has a higher MW and broader MW distribution than CB11, see Table 6.3. Therefore, this must be the effect of more extensive branching in CB11 than in the others. The differences among CB22, CB3, and CB24 are related to their MW distribution, and G' is higher for the higher \bar{M}_n . This indicates the effect of the low MW fraction on G' .

Figure 6.19 shows $\log G''$ versus $\log G'$ plot for the four samples. The curve of CB11 lies at the right side of those of the others [25].

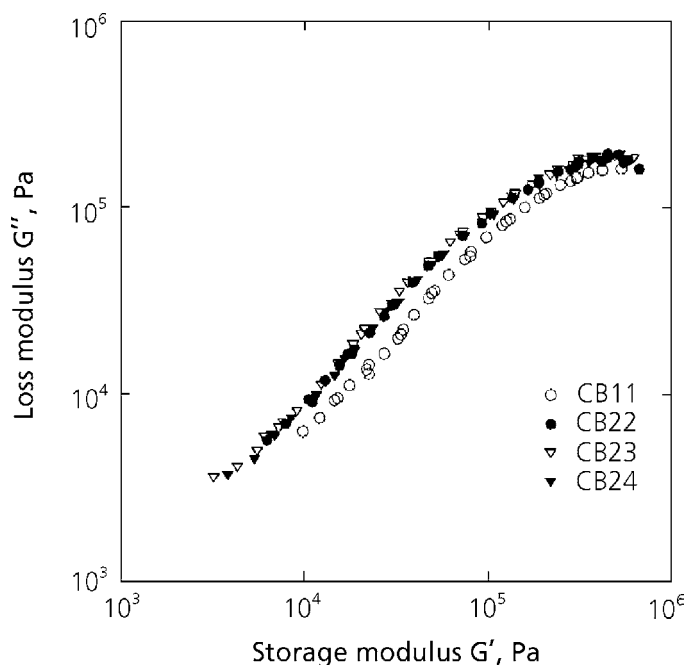


Figure 6.19 Comparison of $\log G''$ versus $\log G'$ curves.

Reprinted from N. Nakajima and Y. Yamaguchi, *Journal of Applied Polymer Science*, 1996, 61, 9, 1525. Copyright 1996, reprinted by permission of John Wiley and Sons, Inc.

The values of the shift factors, a_T and β_T are given in Table 6.4. The a_T s are sample-dependent and CB11, which has the highest degree of branching, shows the highest temperature dependence. At the lower temperature CB24 shows a lower temperature dependence than CB22 and CB23. However, the differences diminish at the higher temperature. The fact that the differences of a_T diminish at the higher temperature indicates that the constraints introduced by the branching become less effective at the higher temperature. The observed β_T values, Table 6.4, are comparable to the values of $\rho_0 T_0 / \rho T$.

No further significant information was obtained from β_T . From the results mentioned above, (see Figure 6.19 and Table 6.3), the order of degree of branching is $\text{CB11} > \text{CB22} = \text{CB23} > \text{CB24}$. Figure 6.20 shows the absolute values of complex viscosity $|\eta^*|$ of the samples at 30 °C.

As observed in many commercial rubbers, these do not show the Newtonian region within the observed time scale because of their high MW, broad MW distribution, and branching. At low frequencies, they show the viscosity enhancement resulting from branching, which is longer than the critical length [25]. The sample of CB11, in spite of having the same \overline{M}_w as those of CB22 and CB23, shows the highest degree of the viscosity enhancement at low frequencies and viscosity reduction at high frequencies; that is the curve of CB11 crosses over the other curves. This also indicates that CB11 has more extensive branching compared to other samples [25]. For CB22, CB23 and CB24 the magnitude of $|\eta^*|$ is in the order of number average MW, \overline{M}_n , see Table 6.3.

Table 6.4 Shift Factors, a_T and β_T					
Temperature (°C) Sample	30	60	90	120	150
a_T					
CB11	1	0.368	0.171	0.094	0.052*
CB22	1	0.409	0.202	0.124	0.071*
CB23	1	0.400	0.202	0.111	0.066
CB24	1	0.449	0.215	0.117	0.067*
β_T					
CB11	1	0.934	0.834	0.794	–
CB22	1	0.910	0.803	0.753	–
CB23	1	0.893	0.844	0.734	0.660
CB24	1	0.938	0.828	0.726	–
$\rho_0 T_0 / \rho T$	1	0.910	0.835	0.771	0.716
*Slight degradation was noticed.					

- *Tensile stress-strain measurements*

Figures 6.21 and 6.22 show tensile stress-strain curves of CB11 and CB24 at various deformation rates. The filled circles show the data at break. Reproducibility shown in the figures is less than $\pm 15\%$. The modulus increases with increasing deformation rates.

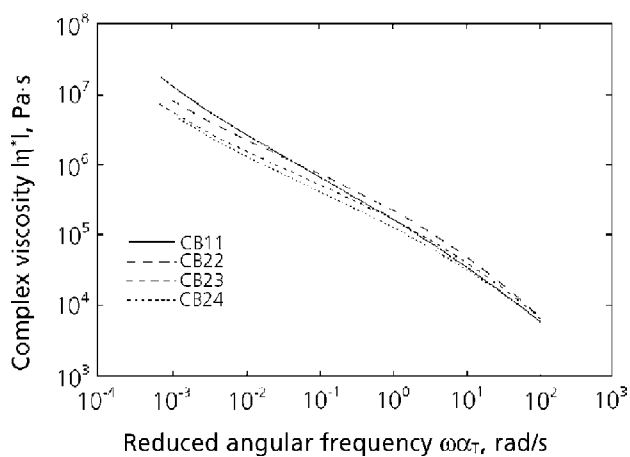


Figure 6.20 Comparison of master curves of complex viscosity of BUNA samples (reference temperature 30 °C).

Reprinted from N. Nakajima and Y. Yamaguchi, *Journal of Applied Polymer Science*, 1996, 61, 9, 1525. Copyright 1996, reprinted by permission of John Wiley and Sons, Inc.

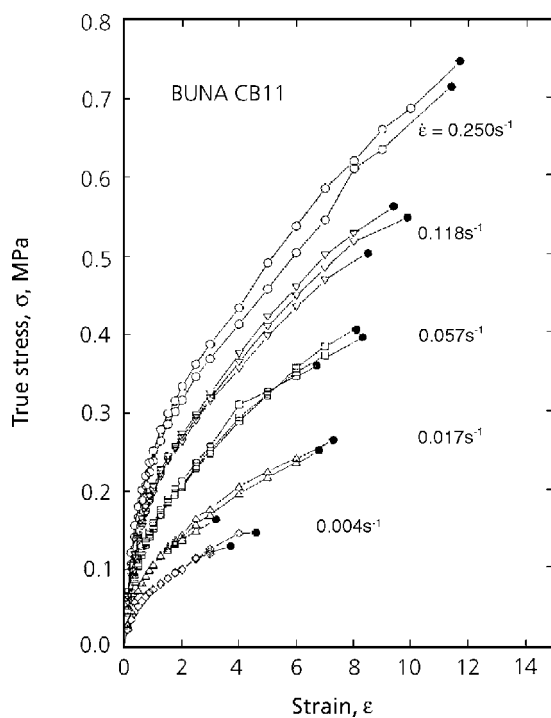


Figure 6.21 Tensile stress-strain curves of BUNA CB11.

Reprinted from N. Nakajima and Y. Yamaguchi, *Journal of Applied Polymer Science*, 1996, 61, 9, 1525. Copyright 1996, reprinted by permission of John Wiley and Sons, Inc.

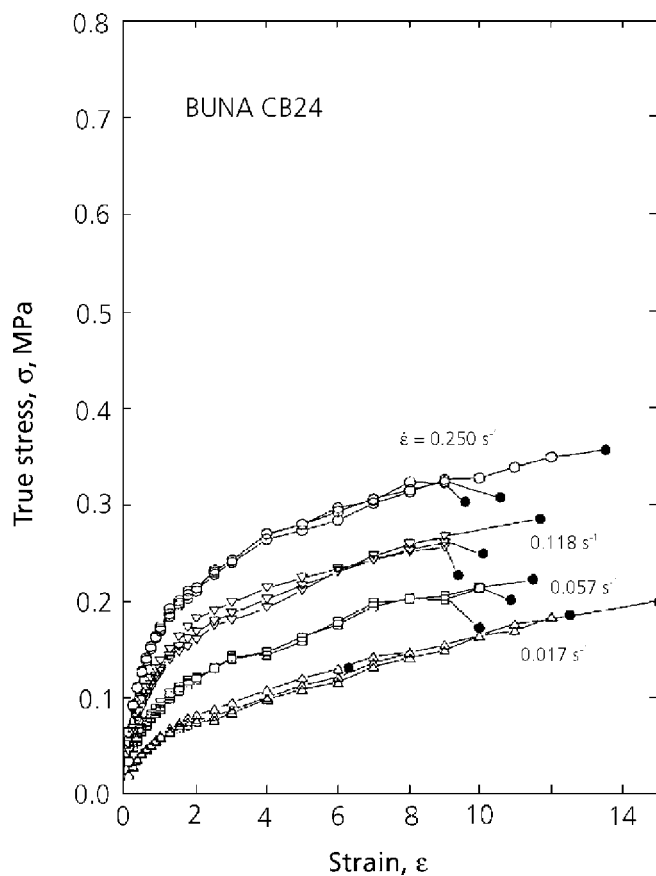


Figure 6.22 Tensile stress-strain curves of BUNA CB24.

Reprinted from N. Nakajima and Y. Yamaguchi, *Journal of Applied Polymer Science*, 1996, 61, 9, 1525. Copyright 1996, reprinted by permission of John Wiley and Sons, Inc.

Figure 6.23 shows the plots of tensile modulus, $E(t)$, against time, t , at various deformation rates for CB24. The data obtained at different deformation rates do not give a master curve, because the behaviour is not linearly viscoelastic [7].

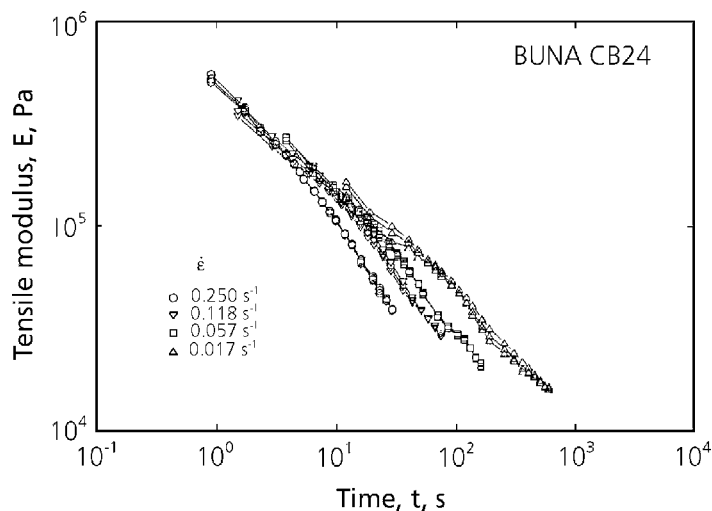


Figure 6.23 Tensile modulus as a function of time for BUNA CB24.

Reprinted from N. Nakajima and Y. Yamaguchi, *Journal of Applied Polymer Science*, 1996, 61, 9, 1525. Copyright 1996, reprinted by permission of John Wiley and Sons, Inc.

Figures 6.24-6.26 show the plots of tensile modulus, $E(\alpha t)$, against reduced time, αt , as given by Equation 6.27.

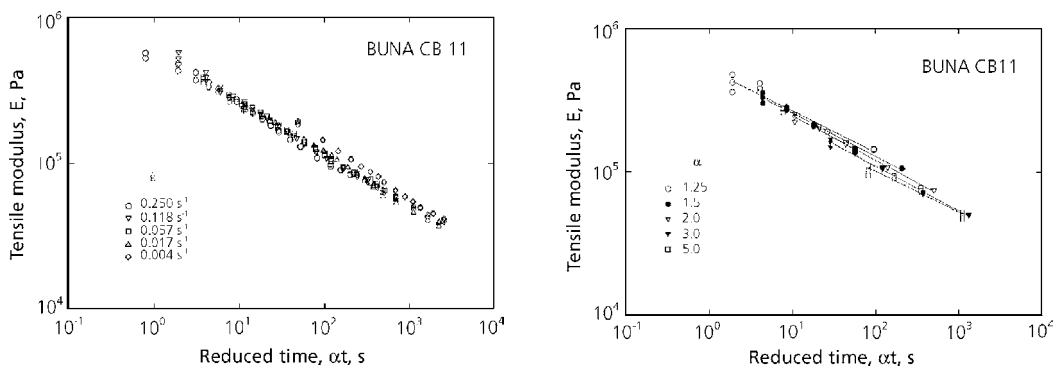


Figure 6.24 a) Tensile modulus as a function of reduced time at fixed rates for BUNA CB11.
b) Tensile modulus as a function of reduced time at fixed extension ratios for BUNA CB11.

Reprinted from N. Nakajima and Y. Yamaguchi, *Journal of Applied Polymer Science*, 1996, 61, 9, 1525. Copyright 1996, reprinted by permission of John Wiley and Sons, Inc.

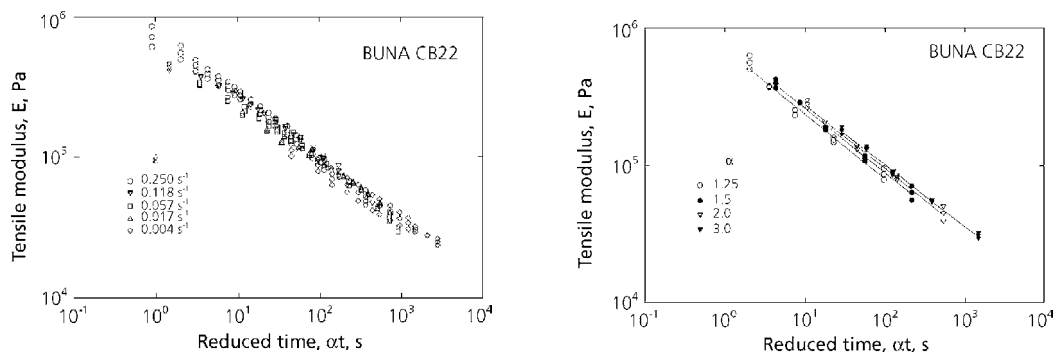


Figure 6.25 a) Tensile modulus as a function of reduced time at fixed rates for BUNA CB22.
b) Tensile modulus as a function of reduced time at fixed extension ratios for BUNA CB22.

Reprinted from N. Nakajima and Y. Yamaguchi, *Journal of Applied Polymer Science*, 1996, 61, 9, 1525. Copyright 1996, reprinted by permission of John Wiley and Sons, Inc.

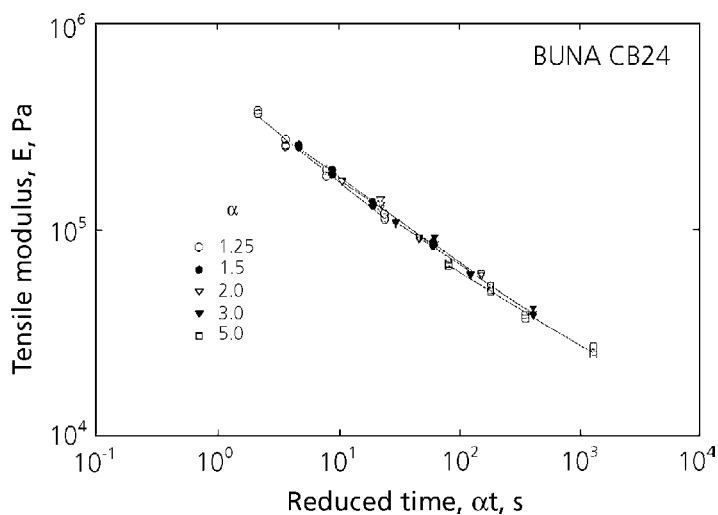


Figure 6.26 Tensile modulus as a function of reduced time at fixed extension ratios for BUNA CB24.

Reprinted from N. Nakajima and Y. Yamaguchi, *Journal of Applied Polymer Science*, 1996, 61, 9, 1525. Copyright 1996, reprinted by permission of John Wiley and Sons, Inc.

In Figures 6.24 (a) and 6.25 (a) the data are plotted for each strain rate, and in Figures 6.24 (b), 6.25 (b) and 6.26 the lines are for constant values of α . CB11 and CB22 show a systematic relationship with α , while CB24 gives a master curve which is independent of α . With CB11 the deviation is in the direction of strain-softening and for CB22 and CB23 it is strain-hardening. Among CB22, CB23, and CB24 the extent of the strain-hardening relates to the amount of branching given in Table 6.3. Even though CB11 has the highest amount of branching, it shows strain-softening behaviour. It should be noted that CB11 is made with a catalyst system different from that used for the other systems, see Table 6.3. Evidently, the branches of the polymer are not long enough to provide the constrained entanglement upon stretching.

When the modulus shift [32], Equation 6.28, is applied, master curves are formed for CB11, CB22, and CB23. Figure 6.27 shows the result for CB22.

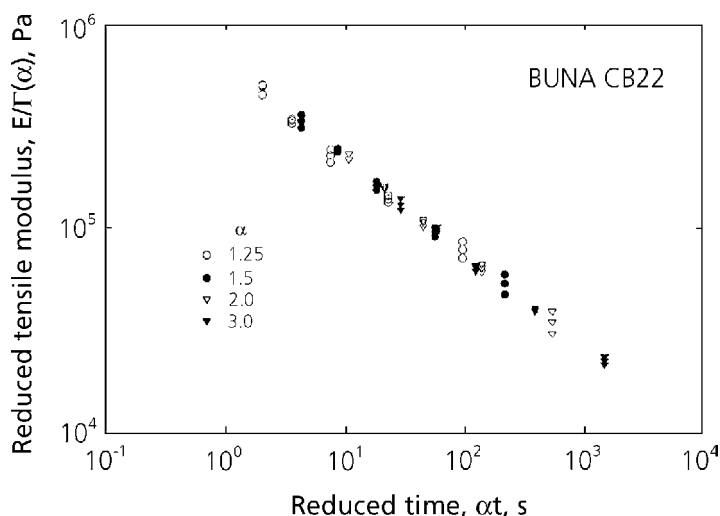


Figure 6.27 Reduced tensile modulus as a function of reduced time for BUNA CB22.

Reprinted from N. Nakajima and Y. Yamaguchi, Journal of Applied Polymer Science, 1996, 61, 9, 1525. Copyright 1996, reprinted by permission of John Wiley and Sons, Inc.

With the emulsion-polymerised rubbers, the modulus shift is required only when an extensive amount of macrogel is present [22]. However, there is no gel in the samples referred to in this work. This is the only time when strain hardening was observed for the sample containing no gel. It implies that the long branches in these BRs are very long.

Figure 6.28 shows the modulus shift, $\Gamma(\alpha)$, for the samples of CB11, CB22 and CB23 as a function of extension ratio.

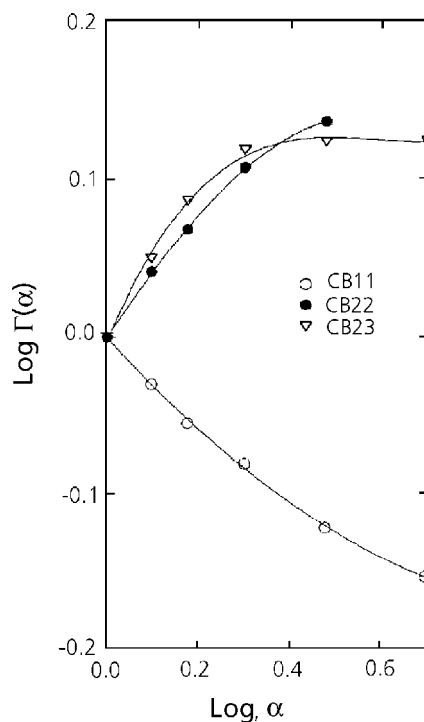


Figure 6.28 Modulus shift factor as a function of extension ratio.

Reprinted from N. Nakajima and Y. Yamaguchi, Journal of Applied Polymer Science, 1996, 61, 9, 1525. Copyright 1996, reprinted by permission of John Wiley and Sons, Inc.

In this figure, no data for CB24 are shown. Although CB24 has long branching, it shows neither strain-hardening nor strain-softening. This indicates that it has the critical length of branching bordering strain-hardening and strain-softening. At this critical branch-length, branches no longer contribute to such behaviour as strain-hardening or strain-softening.

Figures 6.29-6.32 show the comparison between the complex viscosity, $|\eta^*|$, and the equivalent shear viscosity, η_T calculated from the tensile stress-strain data.

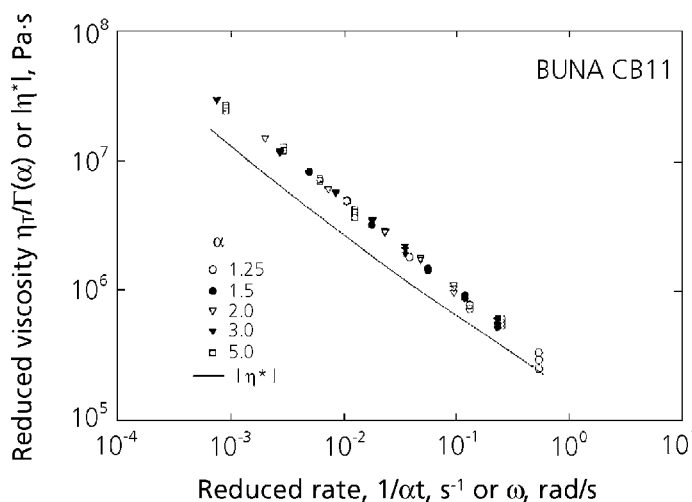


Figure 6.29 Comparison of complex shear viscosity with corresponding viscosity calculated from tensile data for BUNA CB11.

Reprinted from N. Nakajima and Y. Yamaguchi, *Journal of Applied Polymer Science*, 1996, 61, 9, 1525. Copyright 1996, reprinted by permission of John Wiley and Sons, Inc.

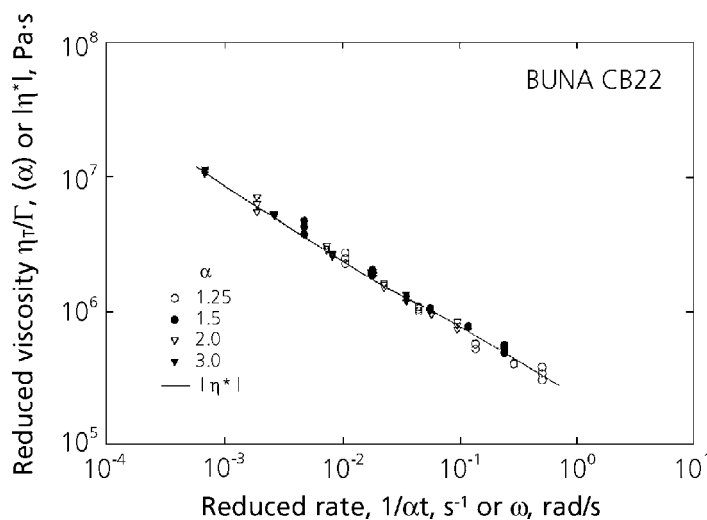


Figure 6.30 Comparison of complex shear viscosity with corresponding viscosity calculated from tensile data for BUNA CB22.

Reprinted from N. Nakajima and Y. Yamaguchi, *Journal of Applied Polymer Science*, 1996, 61, 9, 1525. Copyright 1996, reprinted by permission of John Wiley and Sons, Inc.

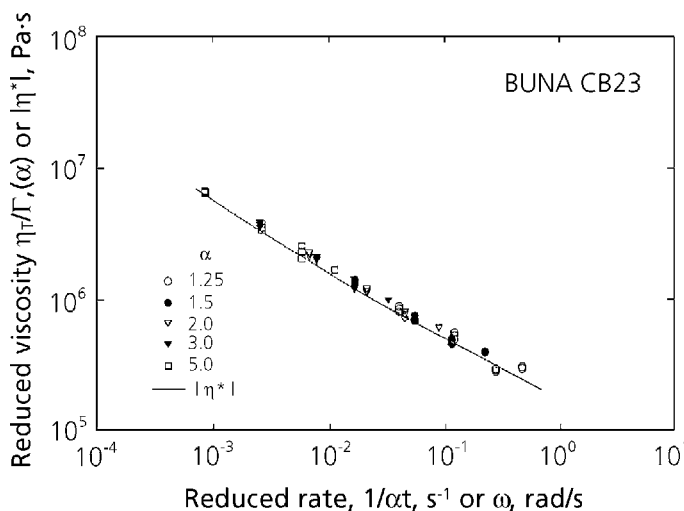


Figure 6.31 Comparison of complex shear viscosity with corresponding viscosity calculated from tensile data for BUNA CB23.

Reprinted from N. Nakajima and Y. Yamaguchi, *Journal of Applied Polymer Science*, 1996, 61, 9, 1525. Copyright 1996, reprinted by permission of John Wiley and Sons, Inc.

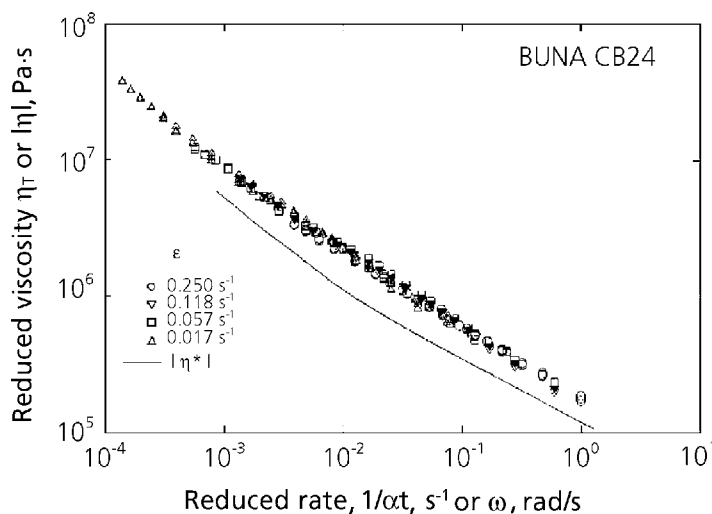


Figure 6.32 Comparison of complex shear viscosity with corresponding viscosity calculated from tensile data for BUNA CB24.

Reprinted from N. Nakajima and Y. Yamaguchi, *Journal of Applied Polymer Science*, 1996, 61, 9, 1525. Copyright 1996, reprinted by permission of John Wiley and Sons, Inc.

The calculation of η_T for CB11, CB 22, and CB23 includes the modulus shift. The values of η_T are higher than those of $|\eta^*|$ for CB11 and CB24. These results indicate that the deformational modes are different for shear and extension. The η_T for CB11 and CB24 tends to converge with $|\eta^*|$ at the higher reduced rate, ie., at smaller deformation. With CB22 and CB23, the values of η_T agree with $|\eta^*|$. The above disagreement between η_T and $|\eta^*|$ indicates strain-induced crystallisation at the larger deformation. The rubber, CB11, was previously shown to give the strain-softening, and CB 24 neither softening nor hardening. The implication is that easily stretchable rubbers crystallise more easily upon straining. At present we do not know why strain-induced crystallisation does not appear as strain-hardening. The results of this work show that the effect of branching and that of strain-induced crystallisation are observable separately, the fact which is an obvious advantage in analysing the behaviour.

- *Experiment-II* [33]
- *Samples*

The samples used were four commercial polybutadienes, UBEPOL-VCR, produced by UBE Industries, see Table 6.5.

Table 6.5 Properties of UBEPOL-VCR Polybutadienes				
Sample	VCR309 ^a	VCR412 ^a	VCR617 ^a	VCR512 ^a
Catalyst	Co	Co	Co	Co
$\bar{M}_w 10^{-4}$ ^b	45.9	45.1	46.2	44.2
$\bar{M}_n 10^{-4}$ ^b	17.1	18.4	17.6	15.5
\bar{M}_w/\bar{M}_n ^b	2.7	2.5	2.6	2.9
SPB ^c (wt%)	9	12	17	12
MV ^d	39	45	63	43
Data supplied by the manufacturer a: Registered trademark of UBE Industries b: Data obtained by GPC; MW are not absolute but relative values based on the hydrodynamically equivalent volume of PS standards. The data represent the matrix polymer only. c: The amount of syndiotactic 1,2-polybutadiene crystalline particles d: Mooney Viscosity				

These rubbers contain crystalline particles of syndiotactic 1,2-polybutadiene in the matrix polymer of *cis*-1,4-BR. The crystalline particle is composed of block copolymers of *cis*-1,4 butadiene/1,2-vinyl butadiene [34]. It has 80% crystallinity in the 1,2-polybutadiene domain and a melting point of 204 °C. The rubbers of VCR309, VCR412, and VCR617 have different amount of crystalline particles in the same matrix polymer. Although not shown in Table 6.5, VCR512 has a different matrix polymer that is more branched than the matrix polymer of other samples.

- *Results and discussion*
- *Oscillatory shear measurements*

The results of time-temperature superposition are shown in Figures 6.33 to 6.36, where all the data were reduced to 30 °C. All curves approach the plateau region at the higher frequencies.

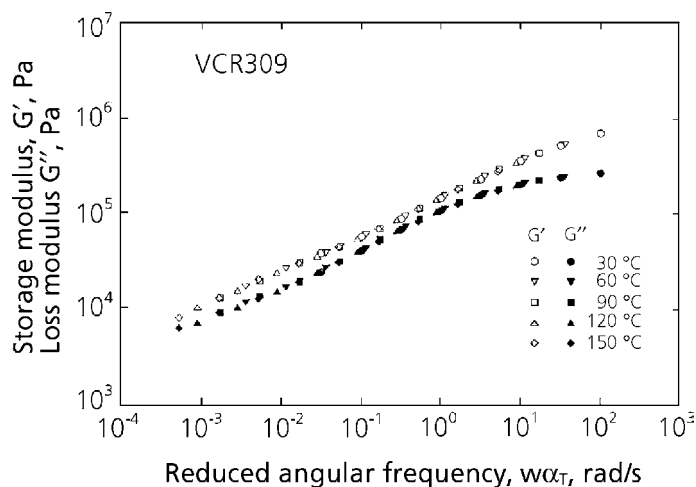


Figure 6.33 Master curves of storage and loss modulus of VCR309 (reference temperature is 30 °C).

Reprinted from N. Nakajima and Y. Yamaguchi, *Journal of Applied Polymer Science*, 1996, 62, 13, 2329. Copyright 1996, reprinted by permission of John Wiley and Sons, Inc.

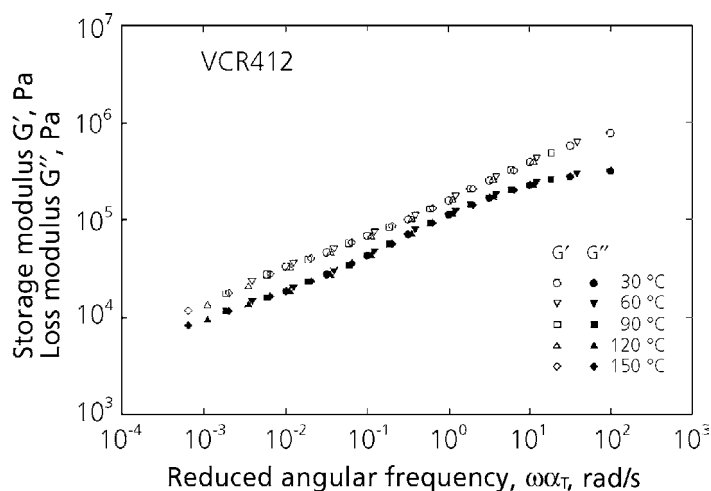


Figure 6.34 Master curves of storage and loss modulus of VCR412 (reference temperature is 30 °C).

Reprinted from N. Nakajima and Y. Yamaguchi, *Journal of Applied Polymer Science*, 1996, 62, 13, 2329. Copyright 1996, reprinted by permission of John Wiley and Sons, Inc.

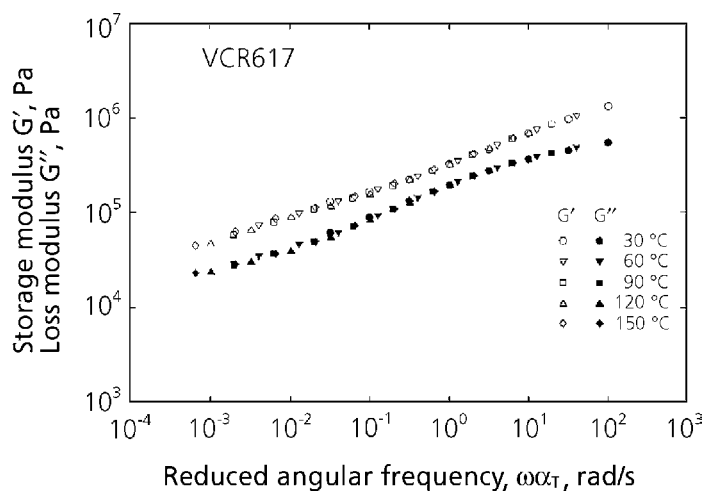


Figure 6.35 Master curves of storage and loss modulus of VCR617 (reference temperature is 30 °C).

Reprinted from N. Nakajima and Y. Yamaguchi, *Journal of Applied Polymer Science*, 1996, 62, 13, 2329. Copyright 1996, reprinted by permission of John Wiley and Sons, Inc.

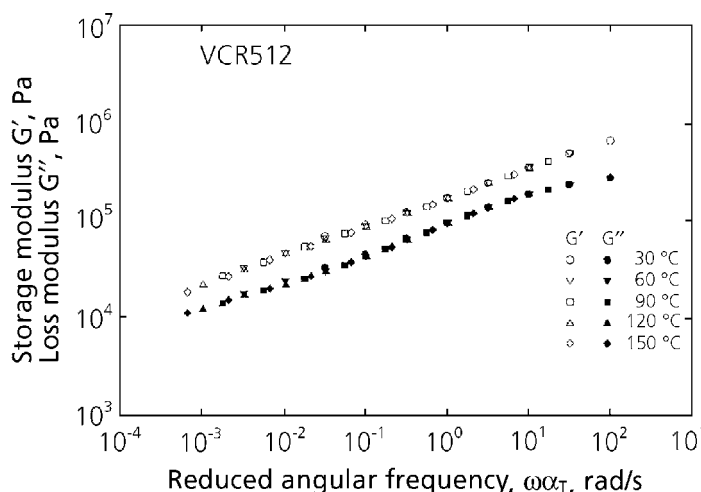


Figure 6.36 Master curves of storage and loss modulus of VCR512 (reference temperature is 30 °C).

Reprinted from N. Nakajima and Y. Yamaguchi, Journal of Applied Polymer Science, 1996, 62, 13, 2329. Copyright 1996, reprinted by permission of John Wiley and Sons, Inc.

However, these curves do not show the cross over of G' and G'' . They are almost parallel to each other. This is because of the presence of the crystalline particles and branching in the matrix polymer.

Figure 6.37 shows $\log G''$ versus $\log G'$ plot for all four rubbers.

The curves shift to the right with an increasing amount of crystalline particles. This indicates that the rubber becomes more elastic in the presence of the particles. The curve of VCR512 lies at the right side of that of VCR412 because the matrix polymer of the former is more branched than the matrix of the latter. The values of the shift factors, a_T and β_T are given in Table 6.6.

The a_T s are sample dependent, and VCR309, which has the least amount of the crystalline particles, shows the highest temperature dependence among the rubber having the same matrix polymer. The rubber with a more branched matrix, VCR512, shows somewhat higher temperature dependence than that of VCR412. However, the differences of a_T diminish at the higher temperature. The observed values of β_T , see Table 6.6, are comparable to the values of $\rho_0 T_0 / \rho T$. The temperature dependence of β_T decreases with the increasing particle content, and it almost disappears for VCR 617 between 30 and 90 °C. This may be the result of the difference in the thermal expansion coefficients of the matrix rubber and the crystalline particle.

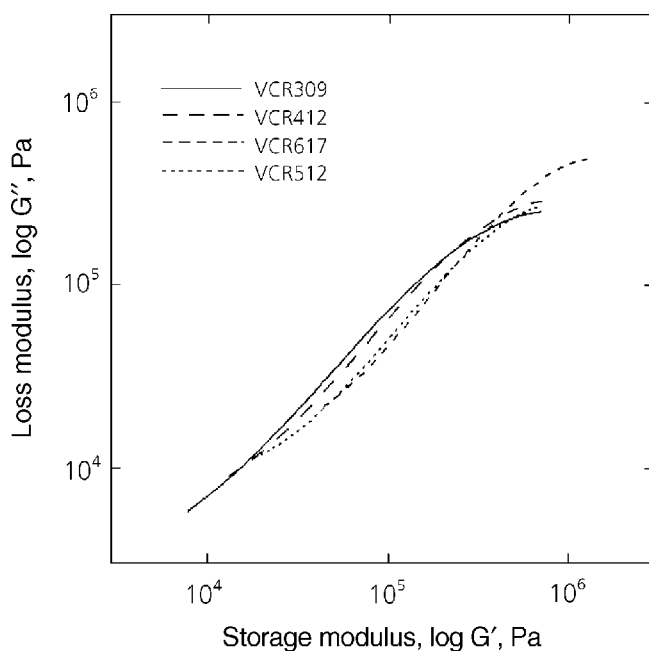


Figure 6.37 Comparison of $\log G''$ versus $\log G'$ curves.

Reprinted from N. Nakajima and Y. Yamaguchi, *Journal of Applied Polymer Science*, 1996, 62, 13, 2329. Copyright 1996, reprinted by permission of John Wiley and Sons, Inc.

Table 6.6 Shift Factors, a_T and β_T					
Temperature (°C) Sample	30	60	90	120	150
a_T					
VCR309	1	0.360	0.171	0.089	0.052
VCR412	1	0.388	0.186	0.111	0.064
VCR617	1	0.404	0.195	0.102	0.065
VCR512	1	0.325	0.178	0.104	0.067
β_T					
VCR309	1	0.906	0.830	0.731	0.665
VCR412	1	0.971	0.889	0.839	0.793
VCR617	1	1.000	1.000	0.879	0.855
VCR512	1	0.859	0.849	0.774	0.714
$\rho_0 T_0 / \rho T$	1	0.910	0.835	0.771	0.716

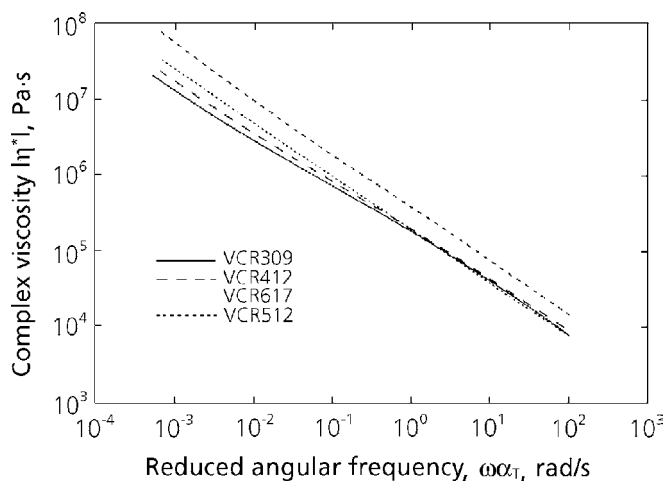


Figure 6.38 Comparison of master curves of complex viscosity VCR412 (reference temperature is 30 °C).

Reprinted from N. Nakajima and Y. Yamaguchi, Journal of Applied Polymer Science, 1996, 62, 13, 2329. Copyright 1996, reprinted by permission of John Wiley and Sons, Inc.

Figure 6.38 shows the absolute values of complex viscosity $|\eta^*|$ of the rubber at 30 °C. As observed in many commercial rubbers, these do not show the Newtonian region within the observed time scale because of their high MW, broad MW distribution, branching and the presence of the particles. Among VCR309, VCR412, and VCR617, the value of $|\eta^*|$ is higher for larger amount of the crystalline particles. At low frequencies, viscosity enhancement increases with increasing amount of crystalline particles. This is similar to the effect of the dispersed particles on viscosity. At low frequencies, the viscosity of VCR512 is higher than that of VCR412. As the frequency is increased, the curve of VCR512 crosses over the curve of VCR412. This is the result of VCR512 having more extensive branching than VCR412.

- *Tensile stress-strain measurements*

Figures 6.39 and 6.40 show tensile stress-strain curves of VCR412 and VCR617 at various deformation rates.

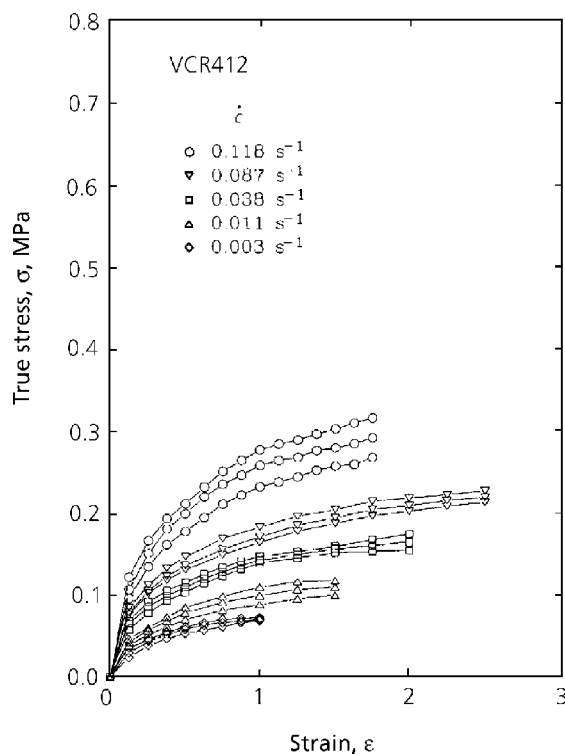


Figure 6.39 Tensile stress-strain curves of VCR412.

Reprinted from N. Nakajima and Y. Yamaguchi, *Journal of Applied Polymer Science*, 1996, 62, 13, 2329. Copyright 1996, reprinted by permission of John Wiley and Sons, Inc.

The stress σ is the true stress based on the deformed cross-section. Reproducibility shown in the figures is less than $\pm 15\%$. The modulus increases with increasing deformation rates. It is higher for the higher amount of the crystalline particles. The stress-strain curves of the other samples are similar to those shown in Figures 6.39 and 6.40.

Figure 6.41 shows the plots of tensile modulus $E(\alpha t)$ against reduced time αt for VCR412, as given by Equation 6.27.

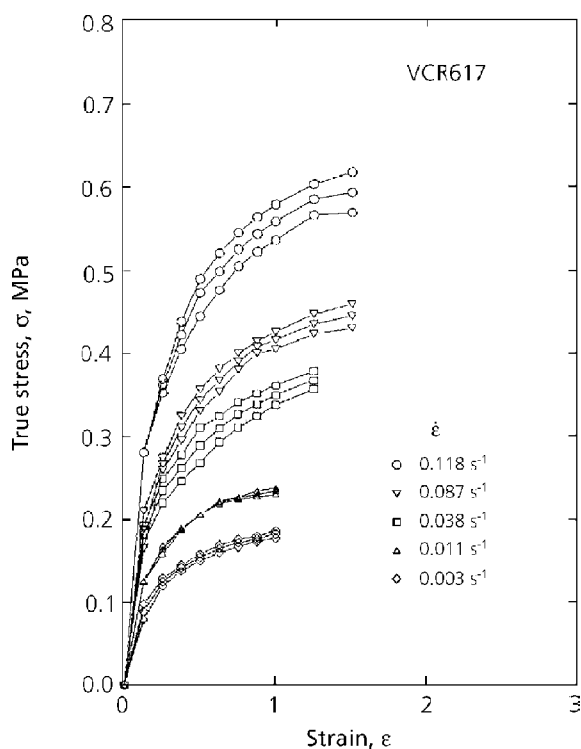


Figure 6.40 Tensile stress-strain curves of VCR617.

Reprinted from N. Nakajima and Y. Yamaguchi, *Journal of Applied Polymer Science*, 1996, 62, 13, 2329. Copyright 1996, reprinted by permission of John Wiley and Sons, Inc.

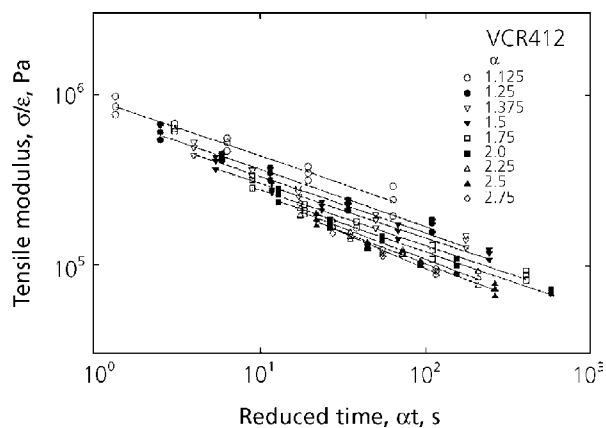


Figure 6.41 Tensile modulus as a function of reduced time at fixed extension ratios for VCR412.

Reprinted from N. Nakajima and Y. Yamaguchi, *Journal of Applied Polymer Science*, 1996, 62, 13, 2329. Copyright 1996, reprinted by permission of John Wiley and Sons, Inc.

In this figure, the lines connect the data at a constant value of α . Instead of forming a master curve, the data systematically change with α . The deviation is in the direction of strain-softening.

When the modulus shift, Equation 6.29 is applied, and master curves are formed for all rubbers, as in Figure 6.42 for VCR412.

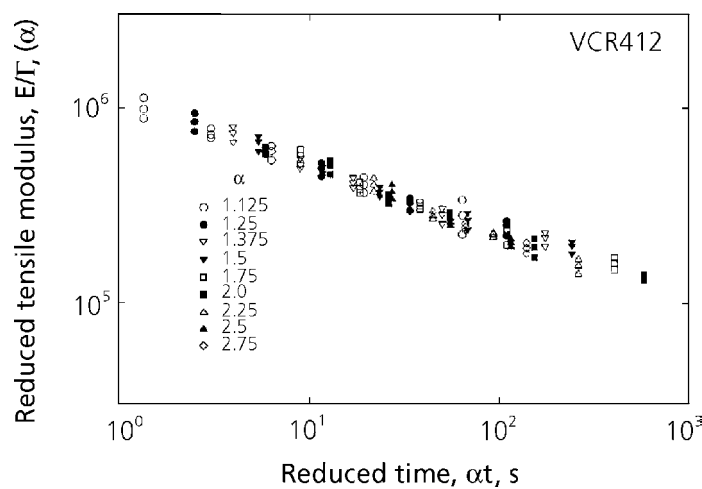


Figure 6.42 Reduced tensile modulus as a function of reduced time for VCR412.

Reprinted from N. Nakajima and Y. Yamaguchi, *Journal of Applied Polymer Science*, 1996, 62, 13, 2329. Copyright 1996, reprinted by permission of John Wiley and Sons, Inc.

Figure 6.43 shows the modulus shift $\Gamma(\alpha)$ as a function of the extension ratio.

The degree of the strain-softening increases with the increasing amount of the crystalline particles. As mentioned before, the crystalline particles consists of a block copolymer of *cis*-1,4-BR and 1,2-BR, the latter providing a crystalline morphology. The *cis*-1,4 chains presumably cover the surface of the particles, compatibilising the particles with the matrix rubber. A diffused boundary between the particle and the matrix was observed with transmission electron microscopy (TEM) for an ultrathin section [34]. Therefore, the *cis*-1,4 chains are like branches spreading out of the surface of the particles. When the branches are not long enough to give the entanglement constraints, they facilitated stretching by lubrication. Because the crystalline particles confer strain-softening, the branches on the particles are not long enough to give the entanglement constraints. This

is also evident since more particles give more strain-softening. Although VCR512 and VCR412 contain the same amount of the crystalline particles, the latter gives more strain softening than the former. The matrix polymer of VCR512 has longer branches than that of VCR412 such that the branching in the former is giving a constrained entanglement. The consequent strain-hardening tendency somewhat offsets the overall degree of the strain-softening from the crystalline particles.

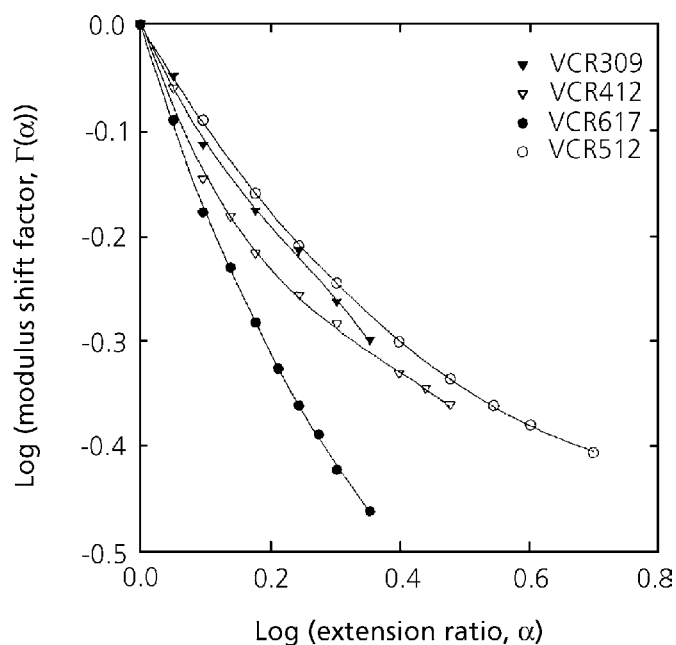


Figure 6.43 Modulus shift factor as a function of extension ratio.

Reprinted from N. Nakajima and Y. Yamaguchi, Journal of Applied Polymer Science, 1996, 62, 13, 2329. Copyright 1996, reprinted by permission of John Wiley and Sons, Inc.

Figures 6.44 to 6.47 show comparisons between the complex viscosity $|\eta^*|$ and the equivalent of shear viscosity η_T , calculated from the tensile stress-strain data.

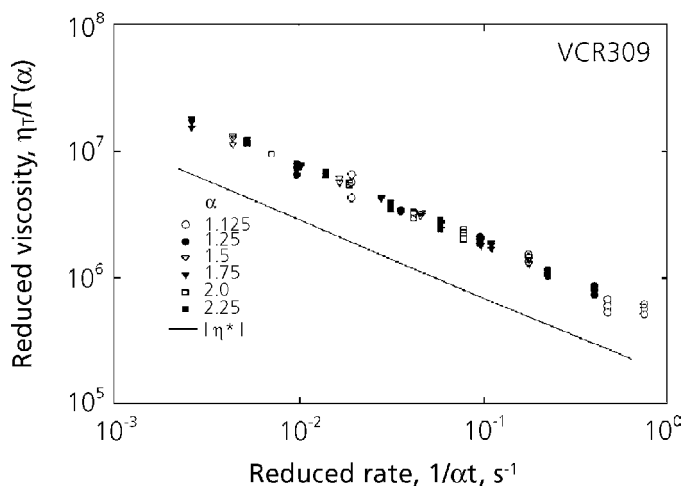


Figure 6.44 Comparison of shear complex viscosity with corresponding viscosity calculated from tensile data for VCR309.

Reprinted from N. Nakajima and Y. Yamaguchi, *Journal of Applied Polymer Science*, 1996, 62, 13, 2329. Copyright 1996, reprinted by permission of John Wiley and Sons, Inc.

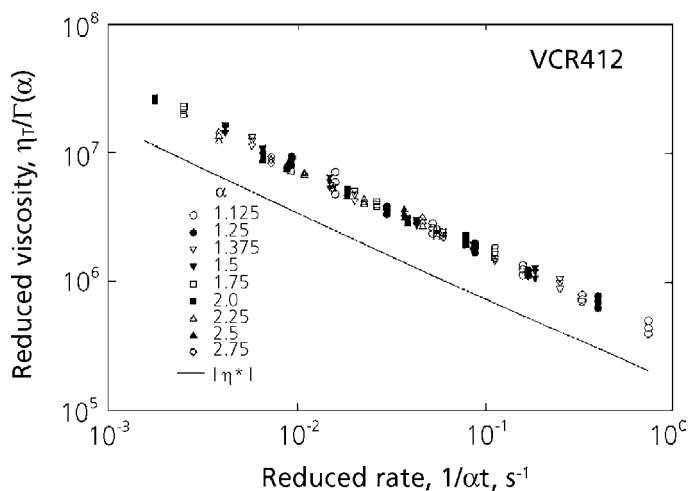


Figure 6.45 Comparison of shear complex viscosity with corresponding viscosity calculated from tensile data for VCR412.

Reprinted from N. Nakajima and Y. Yamaguchi, *Journal of Applied Polymer Science*, 1996, 62, 13, 2329. Copyright 1996, reprinted by permission of John Wiley and Sons, Inc.

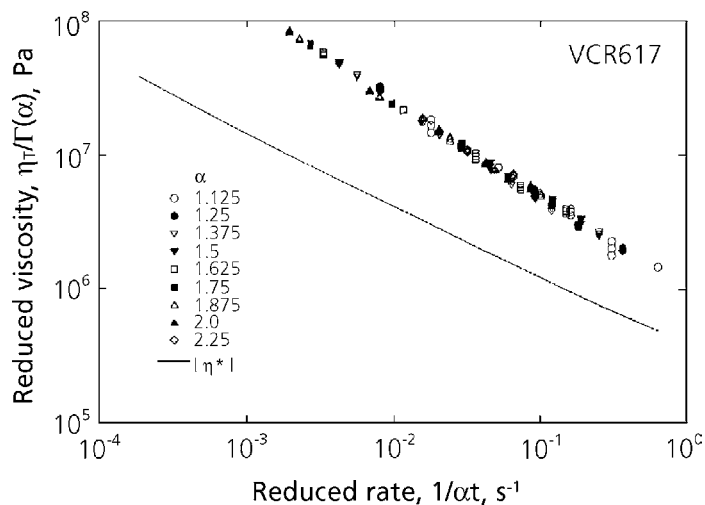


Figure 6.46 Comparison of shear complex viscosity with corresponding viscosity calculated from tensile data for VCR617.

Reprinted from N. Nakajima and Y. Yamaguchi, *Journal of Applied Polymer Science*, 1996, 62, 13, 2329. Copyright 1996, reprinted by permission of John Wiley and Sons, Inc.

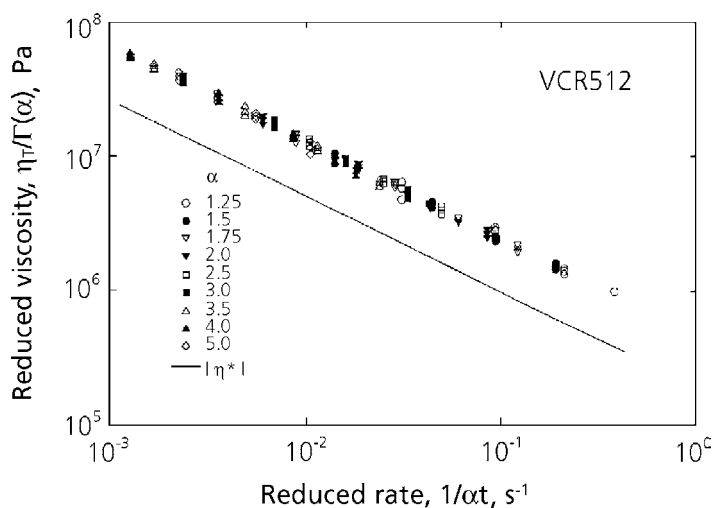


Figure 6.47 Comparison of shear complex viscosity with corresponding viscosity calculated from tensile data for VCR512.

Reprinted from N. Nakajima and Y. Yamaguchi, *Journal of Applied Polymer Science*, 1996, 62, 13, 2329. Copyright 1996, reprinted by permission of John Wiley and Sons, Inc.

The calculation of η_T includes the modulus shift. The curve of η_T is higher than the curves of $|\eta^*|$ for all rubbers. This indicates the strain-induced crystallisation of the matrix polymer at the large elongational deformation. The curves of η_T and $|\eta^*|$ for VCR309, VCR412, and VCR512 are almost parallel to each other. The curves for VCR617 are not parallel, and the difference becomes larger toward lower frequencies. This is because higher crystalline-particle content introduces higher strain-induced crystallisation, and the crystallisation is more significant at the large deformation, which corresponds to the lower frequency in this presentation. In Experiment I as well as this study, the strain-softening was found to facilitate the strain-induced crystallisation. This is contrary to what might be expected from the constraint against elongation, forcing the orientation of the chains, and thus enhancing the crystallisation. The exact mechanism of strain-induced crystallisation requires further study.

- *Experiment-III* [35]
- *Samples*

The gum rubber samples used are listed in Tables 6.3 and 6.5. They may be classified into three groups:

1. Titanium-polymerised rubber, CB11, is the most branched. However, the branches are relatively short. The rubber gives strain-softening and strain-induced crystallisation upon stretching [30].
2. Neodymium-polymerised rubbers, CB22, CB23 and CB24, have low degrees of branching compared to CB11. However, the branches are longer; long enough to give a ‘constrained’ entanglement. It results in strain-hardening when the degree of branching is relatively high, i.e., CB22 and CB23. They do not give strain-induced crystallisation. The least branched rubber, CB24, gave neither softening nor hardening [30], but gave strain-induced crystallisation.
3. Cobalt-polymerised rubbers, VCR309, VCR412, VCR617 and VCR512, contain dispersed crystalline particles of 1,2-polybutadiene [34]. The first three have different amounts of particles in the same matrix rubber. The matrix rubber of VCR512 has more long branches than that of VCR412. The crystalline particles are made up of a block copolymer of *cis*-1,4 and 1,2-butadiene [34]. The crystalline particles cause strain softening. The extent of strain-softening is lessened in VCR512 because the branching of the matrix is long enough to give the ‘constrained’ entanglement resulting in strain-hardening. All VCRs gave strain-induced crystallisation [33].

The compounds were made from these rubbers with the addition of 50 phr N330 carbon black from Cabot.

- *Mixing and milling*

A Banbury-type internal mixer with a 250 ml capacity was used for mixing the compounds. The fill factor was 0.7 and the rotor speed was 100 rpm. After mastication of the rubber for 1 minute, carbon black was added over a period of 1 minute. After an additional 2 minutes, the compound was dumped. All dumped compounds were crumbly and a small amount of the free filler remained. After dumping, the compounds were immediately milled with a 6-inch two-roll mill in order to develop further mixing and to observe mill processability. Photographs (see Figures 6.48-6.57) of the rubber on the mill were taken after milling for 2 minutes. The speed of the fast roll was 28 rpm and the friction ratio was 1:1.26.

- *Results*

When CB11 gum was loaded on the mill, it broke into many pieces, which required recharging. The process was repeated several times until a band was formed. The band was loose and sagging as shown in Figure 6.48(a). After taking the photograph, the band was pushed up against the roll in an attempt to make a tight band. The band sagged again if not pushed up and tore at many places as shown in Figure 6.48(b). The CB11 compound did not make a band and crumbled after passing through mill; therefore, no photograph is shown. With CB22, CB23, and CB24, the gum rubbers formed bands immediately after loading. The bands are as shown in Figures 6.49-6.51. The surface of CB22 had a rough texture, that of CB24 was smooth, and that of CB23 was intermediate. The stickiness was observed with all three, but observed least with CB22, more with CB23, and the most with CB24. When the band was cut and the sheet was pulled, CB22 was the most elastic, giving a large mill-shrinkage. The elasticity decreased in the order from CB22 through CB23 to CB24. The CB22, CB23, and CB24 compounds made smooth bands, which were loose on the mill and sagging somewhat, see Figure 6.52.

VCR309, VCR412, and VRC617 made smooth bands immediately after charging as shown in Figures 6.53-6.55. For VCR512, although it did not break into pieces, the band sagged. When it was pushed against the roll, the band was torn, see Figure 6.56, but the tearing was not as extensive as that in the case of CB11. The bands were not sticky; when the sheet was cut and pulled out, there was no appreciable elastic tension. The VCR309, VCR412, VCR617, and VCR512 compounds made tight bands, of which VCR412 and VCR617 had a slight tear, see Figure 6.57.

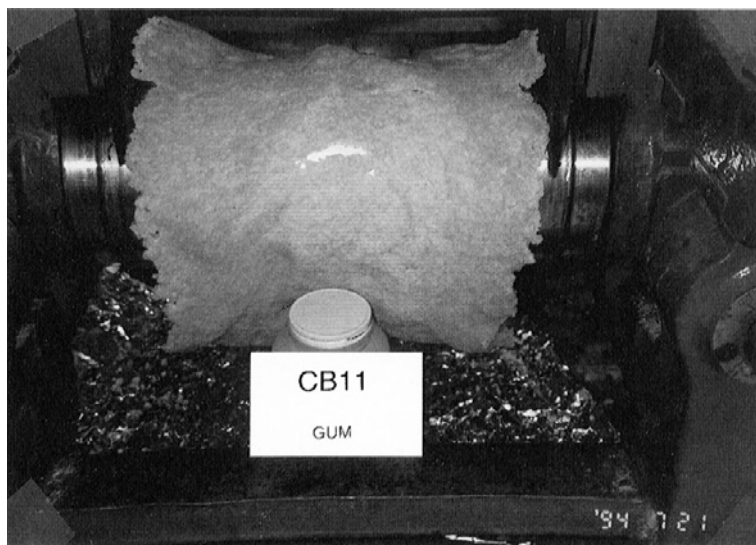


Figure 6.48 a) Photograph of CB11 gum rubber on the mill.

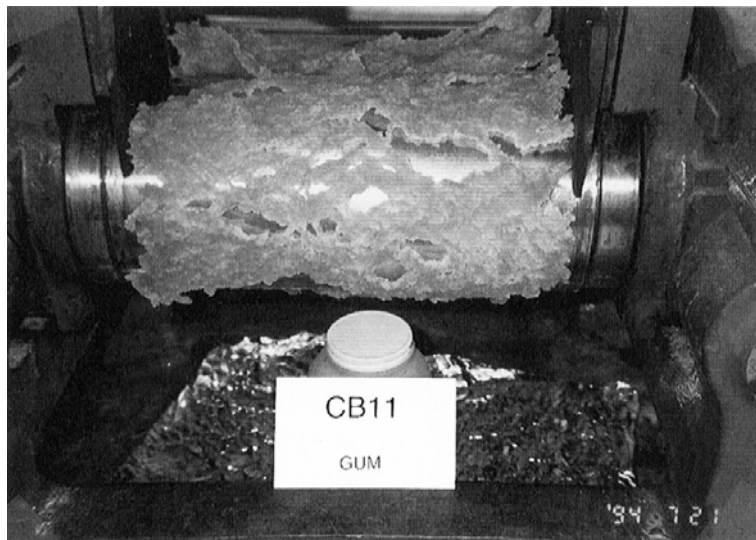


Figure 6.48 b) Photograph of CB11 gum rubber on the mill.

Reprinted from N. Nakajima and Y. Yamaguchi, Journal of Applied Polymer Science, 1997, 65, 10, 1995. Copyright 1997, reprinted by permission of John Wiley & Sons, Inc.

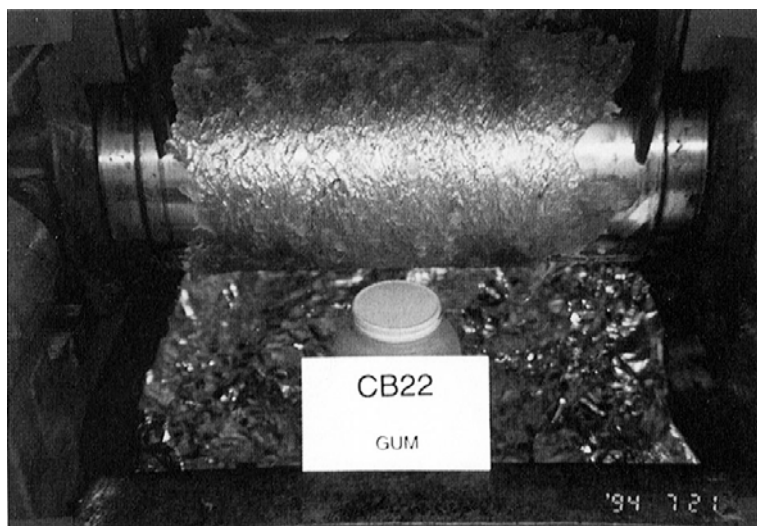


Figure 6.49 Photograph of CB22 gum rubber on the mill.

Reprinted from N. Nakajima and Y. Yamaguchi, Journal of Applied Polymer Science, 1997, 65, 10, 1995. Copyright 1997, reprinted by permission of John Wiley & Sons, Inc.



Figure 6.50 Photograph of CB23 gum rubber on the mill.

Reprinted from N. Nakajima and Y. Yamaguchi, Journal of Applied Polymer Science, 1997, 65, 10, 1995. Copyright 1997, reprinted by permission of John Wiley & Sons, Inc.

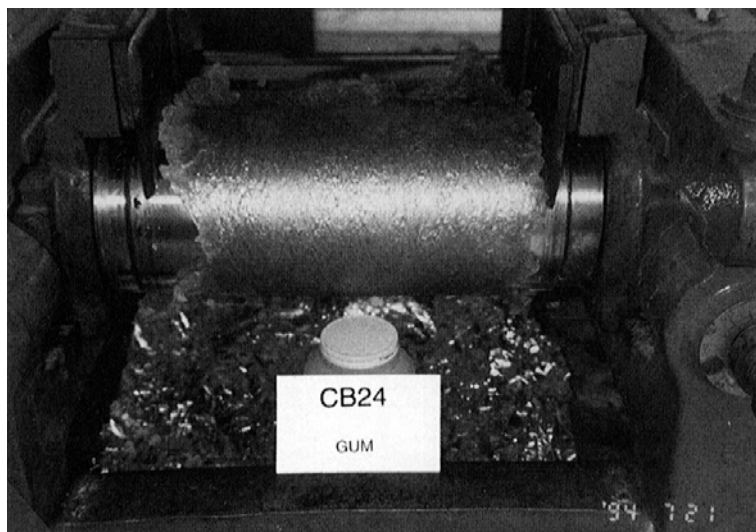


Figure 6.51 Photograph of CB24 gum rubber on the mill.

Reprinted from N. Nakajima and Y. Yamaguchi, Journal of Applied Polymer Science, 1997, 65, 10, 1995. Copyright 1997, reprinted by permission of John Wiley & Sons, Inc.

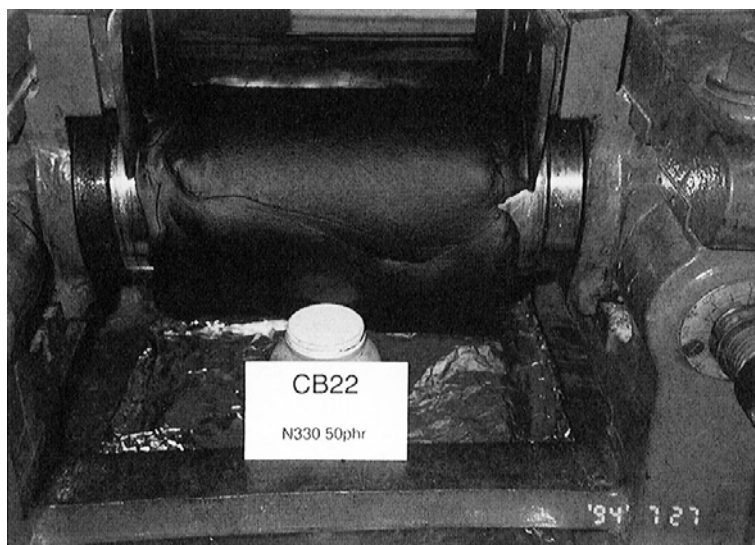


Figure 6.52 Photograph of CB22 carbon black-filled compound on the mill.

Reprinted from N. Nakajima and Y. Yamaguchi, Journal of Applied Polymer Science, 1997, 65, 10, 1995. Copyright 1997, reprinted by permission of John Wiley & Sons, Inc.

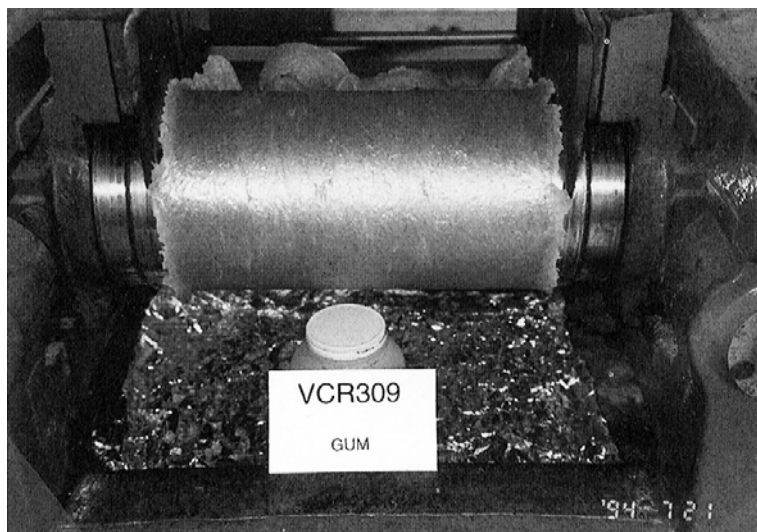


Figure 6.53 Photograph of VCR309 gum rubber on the mill.

Reprinted from N. Nakajima and Y. Yamaguchi, Journal of Applied Polymer Science, 1997, 65, 10, 1995. Copyright 1997, reprinted by permission of John Wiley & Sons, Inc.

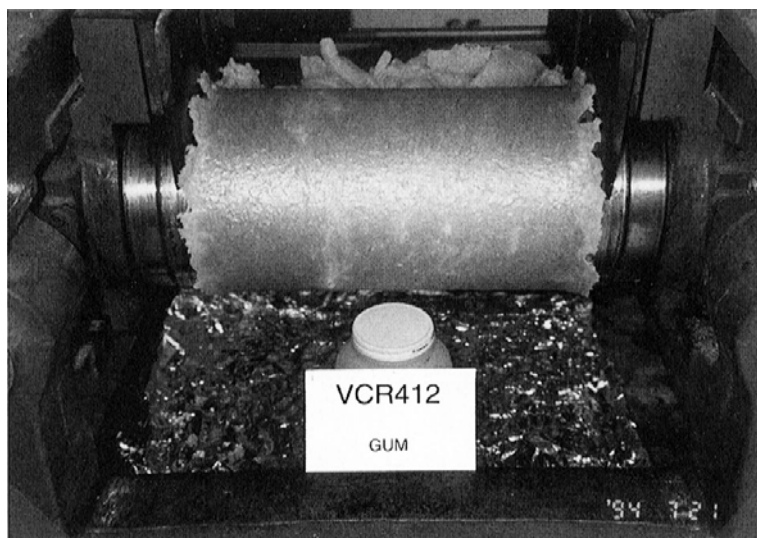


Figure 6.54 Photograph of VCR412 gum rubber on the mill.

Reprinted from N. Nakajima and Y. Yamaguchi, Journal of Applied Polymer Science, 1997, 65, 10, 1995. Copyright 1997, reprinted by permission of John Wiley & Sons, Inc.

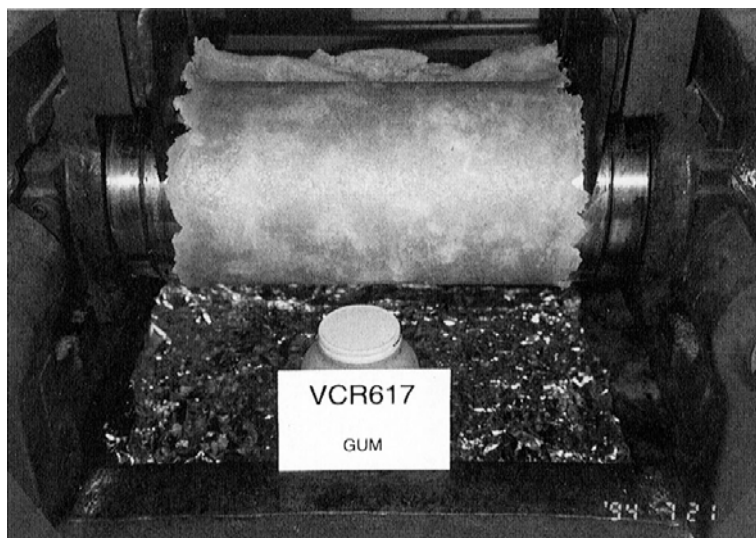


Figure 6.55 Photograph of VCR617 gum rubber on the mill.

Reprinted from N. Nakajima and Y. Yamaguchi, Journal of Applied Polymer Science, 1997, 65, 10, 1995. Copyright 1997, reprinted by permission of John Wiley & Sons, Inc.

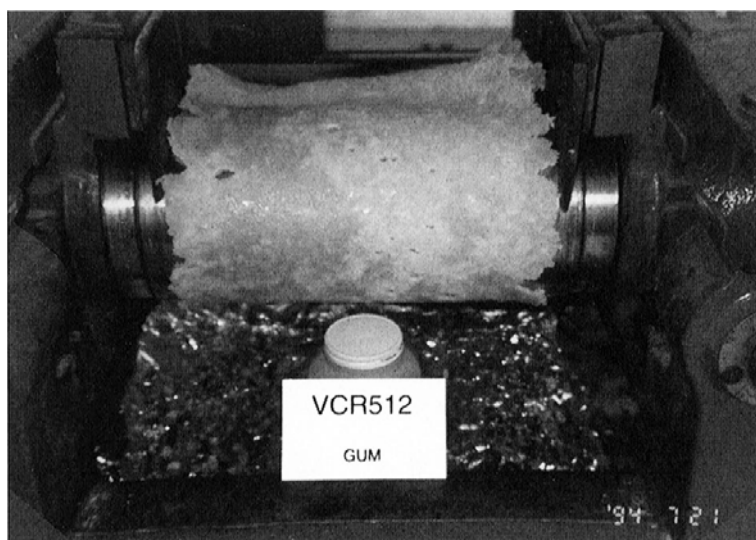


Figure 6.56 Photograph of VCR512 gum rubber on the mill.

Reprinted from N. Nakajima and Y. Yamaguchi, Journal of Applied Polymer Science, 1997, 65, 10, 1995. Copyright 1997, reprinted by permission of John Wiley & Sons, Inc.



Figure 6.57 Photograph of VCR412 carbon black-filled compound on the mill.

Reprinted from N. Nakajima and Y. Yamaguchi, *Journal of Applied Polymer Science*, 1997, 65, 10, 1995. Copyright 1997, reprinted by permission of John Wiley & Sons, Inc.

- *Discussion*

Although CB11 gum broke into many pieces on charging, it is not likely to be processing in Region I, because the rubber is not stiff, and when the band was eventually formed, it behaved more as in processing Region III. If it had been in Region I, it would have moved to Region II eventually. As shown in Figure 6.58, CB11 gum has a rather high rate-dependence (for other CB rubbers, refer to the original articles [30]). From the principle of time-temperature correspondence, we also expect a relatively high temperature dependence. This was already observed in the dynamic measurements [30], where this rubber had highest values of the temperature shift factor, a_T . When the rate decreased, the strain at break decreased significantly, meaning that when the temperature increases, the strain at break also decreases, going into Region III. The high-temperature dependence comes from the high degree of branching. The nature of the difficulties in milling of CB11 gum rubber and its compound are from the same origin. Although CB11 gum rubber gave strain-induced crystallisation in tensile tests, it did not help the processability. When the rubber is in Region III, there is insufficient tension to cause the crystallisation.

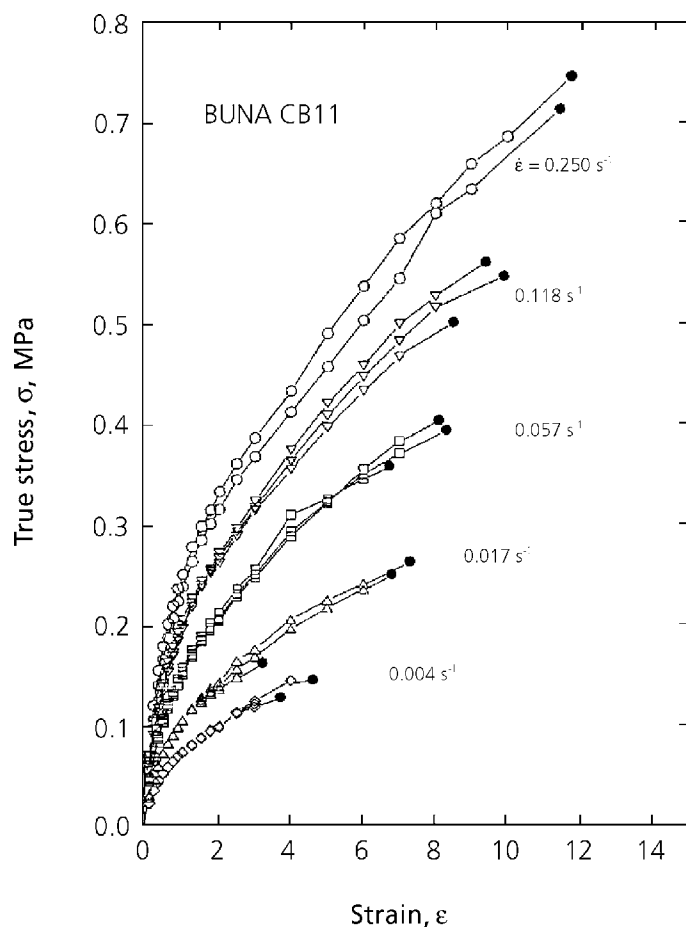


Figure 6.58 Tensile stress-strain curves of CB11 gum rubber.

Reprinted from N. Nakajima and Y. Yamaguchi, *Journal of Applied Polymer Science*, 1997, 65, 10, 1995. Copyright 1997, reprinted by permission of John Wiley & Sons, Inc.

The stickiness of gum rubbers CB22, CB23, and CB24, indicates that they were in Region IV on the mill. When the carbon black was added, stickiness was no longer observed. Because the stickiness was the reason for forming the band in Region IV, the compound became loose from the surface of the roll. Also, in Region IV, there is insufficient tension to cause strain-induced crystallisation for CB24, which crystallises in a tensile test. With VCR309, VCR412, VCR617 and VCR512, the gum rubbers were in Region II, bordering toward Region III, exhibiting slight sagging and tearing in some cases but not sticky. Consequently, the compounds made tight bands, but showed slight tearing. VCR512 gum showed a relatively large rate-dependence in the stress-strain measurement compared to those of other VCRs. This is similar to the behaviour of CB11 as compared to the

other CB rubbers. It implies the higher-temperature dependence as well. This explains the fact that VCR512 tends to move toward Region III as the rubber becomes warmer on the mill. This is seen as a slight sagging and a slight tearing, see Figure 6.56, whereas no sagging or tearing occurred with other VCRs. In contrasting three types of gum rubbers, which are represented by CB11, CB22, and VCR412, a clear-cut differentiation may be made about their mill behaviour. CB11 was in Region III, CB22 type was in Region IV and VCR412 type was in Region II. This ordering is related to the modulus level at the very low frequency region in the dynamic shear measurements [30, 33]. The lower-frequency region of the data represent the higher temperature behaviour, which is encountered in milling. Evidently, the added crystalline particles are most effective in raising the modulus at the low frequency as shown with VCR rubbers. A degree of branching is more effective than is a relative length of branching with respect to the modulus level, CB11 versus CB22. However, if a sticky band, Region IV, is preferred over a sagging band, Region III, CB22 is said to be easier for milling than is CB11.

Among the three neodymium-polymerised rubbers, CB22 had the highest degree of branching, followed by CB23, and CB24 was the least branched. Because branching makes rubber more elastic, it explains the roughest texture and least stickiness of CB22 among the three. CB22 was most elastic when pulled from the mill and showed a large mill shrinkage. The difference in CB23 and CB24 may be explained similarly on the basis of the difference of the degree of branching.

Concerning VCR309, VCR412, and VCR617, there was no significant difference in mill behaviour among these gum rubbers and also among their compounds, meaning that, within the present variation in the amount of the crystalline particles, no difference was detected in the milling. In detail, however, a significant number of white spots appeared in the band of VCR617, a little in that of VCR412, and none in that of VCR309, see Figures 6.53-6.55. The white spots gradually disappeared when the sheets were removed from the mill and left to relax. The white spots appear to be the strain-induced crystalline domains.

Previously, it was noticed with the matrix rubber [33] that in the presence of the larger amount of the crystalline particles there was an indication of more strain-induced crystallisation. Among the samples that we examined, the three rubbers of the VCR series were the only ones, which gave an indication of strain-induced crystallisation in milling. This means that in order for the gum rubber and the compound to have strain-induced crystallisation during milling the material must be under sufficient tension, i.e., Region II.

The mill behaviour of the compounds with respect to the four regions of processability was readily explained from the mill behaviour of the matrix rubber. Within the

structural variables investigated in this study, both gum rubbers and the corresponding compounds were in the same region of mill processability.

6.7.2 Polyethylacrylate

The next example is ACM, which has a rather high T_g of $-14\text{ }^{\circ}\text{C}$, but it tends to fall in the Region III or IV of mill processability, because it is a relatively short and fat molecule. This polymer is made via emulsion polymerisation with a free radical initiator. Therefore, the presence of macrogel is one of the concerns. In one of the samples a difunctional co-monomer was used for providing a cure site. It presents a possibility of forming microgels. Effects of these structural variables on the viscoelastic behaviour and processability are examined.

It is a common occurrence in industry that two elastomers, overall very similar, behave differently on the mill. Sometimes, they are the same grade of material made for the same specification. Other times they are similar but made with some known difference. In either case it is necessary to relate the observed difference in processability with the difference in the molecular architecture of the polymers. Further, such a molecular difference must be related to the difference in the manufacturing process. This work is an example of such an activity, where the rheological analyses have played key roles. Two commercial ACMs, one having an epoxide (EP) crosslinking site and the other ethylidene norbornene (ENB), were used for this study. The dynamic shear oscillation measurements at very small strain were used to characterise the viscoelastic properties. The tensile stress-strain measurements at several different deformation rates were used to characterise the large deformation behaviour. These data were systematically analysed to explain the difference in mill processability. They were also used to pin-point major differences in long branching and gel structure, which impart a dominant influence on rheology and hence, processability. The gel determination was made by filtration in order to support the rheological findings. The dilute solution techniques were not used, because such results would only pertain to the soluble fraction of the polymer.

- *Experimental*
- *Samples*

The samples were two commercial ACMs having a Mooney index of about 50 [14]. The carbon black used for the mill processability was a standard N330 [37]; 50 parts per 100 parts of rubber by weight was used.

The sheets of gum elastomers were prepared in a picture frame between two polished stainless steel plates. The pressing was done at 160 °C for 20 minutes. A mould release agent was used. The sheets were cooled in the press. After removing from the press, the sheets were placed between two steel plates with 10.5 kg weight placed on top. The sheets were allowed to rest for 3 days under the weight to prevent wrinkling. Tensile specimens were cut from the sheets using ASTM D412 dumbbell die C [31].

The gel content of each sample was determined by dissolving about 0.4 g of material in 100 ml of methyl ethyl ketone, and stirring on a magnetic stirrer for 24 hours. The solution was filtered through a Whatman No. 4 filter paper. The filtered paper was weighed before and after filtering to determine the amount of gel removed from the solution. The filtered solution was evaporated and the amount of dissolved polymer was determined. The gel contents before and after pressing are given in Table 6.7.

Table 6.7 Samples and Gel Content		
Sample	Before pressing (% Gel)	After pressing (% Gel)
EP	9.4	15.9
ENB	71.4	66.6

- *Instruments*
- *Viscoelastic measurement*

The viscoelastic properties were measured with a Rheometrics mechanical spectrometer in the oscillation mode. The frequency range was from 10^{-2} to 10^2 rad/s. Samples were tested at 25, 60, 100 and 150 °C.

- *Tensile stress-strain measurement*

Tensile tests were performed on a Monsanto Tensometer 500. The practical upper limit of crosshead speed was 0.847 cm/s and the lower limit was 0.0359 cm/s. The speed was calibrated by measuring with a stopwatch the time required for the crosshead to travel a set distance measured with a measuring tape. This was double checked by measuring the time required to elongate the specimen an additional 100% as measured by the strip chart recorder. A Monsanto extensometer designed for use with the Tensometer 500 was

used to record the strain directly as a percentage. The strip chart recorder was equipped with an area compensator so that all stress data were recorded as force per unit original cross-sectional area of the sample. The force was measured by a 45 kg load cell. The samples were held by roller grips. The tensile test was performed at 25 °C and ambient humidity conditions using strain rates of 0.177, 0.0872, 0.0441 and 0.00775 s⁻¹. These strain rates encompass the practical operating conditions of the tester.

- *Mill processability*

A Stewart-Bolling laboratory mill of 152 mm diameter and 305 mm width, was used to evaluate the mill processability. The speed of the fast roll was 29 rpm and the friction ratio was 1:1.25. The mill rolls were cooled by circulating city water.

- *Results*

Figure 6.59 is the comparison of viscoelastic properties of the two polymers at 25 °C. Both storage modulus, G' and loss modulus, G'' are very similar for the two samples, except at the higher frequency the moduli of the ENB polymer are lower than those of the EP polymer. From this limited data no significant information on the molecular structure can be extracted.

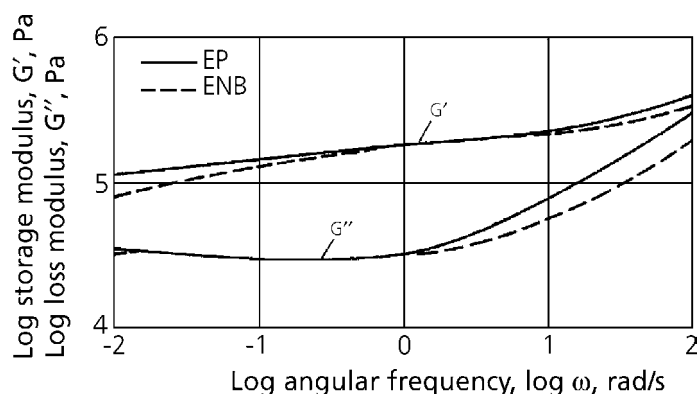


Figure 6.59 Storage and loss modulus of EP and ENB ACM at 25 °C.

Reprinted with permission from N. Nakajima, R. A. Miller and E. R. Harrell, International Polymer Processing, 1987, 2, 2, 87. Copyright 1987, Hanser Publishers.

Figures 6.60 and 6.61 are G' and G'' curves which are extended to lower frequencies with the aid of the temperature reduction scheme [6] using the data obtained at 60, 100 and 150 °C. At the reduced frequency, lower than 10⁻³ rad/s, there are significant differences in the behaviour of two samples. The G' and G'' curves of the EP polymer

begins to turn downward and assume a slope higher than those of the ENB polymer. This indicates that there are differences in the size and amount of the largest species contained in the samples. Here, the term, species, is used instead of MW in order to include gels. Another important difference is that the G' and G'' curves of the EP polymer cross over, G' becoming lower than G'' at $\omega < 10^{-5}$ rad/s. However, with the ENB polymer the G' is above G'' and the two curves are almost parallel to each other. This behaviour indicates that the ENB polymer contains much more gel than the EP polymer. The gel-content data in Table 6.7 support this finding. Figure 6.62 shows log G'' versus log G' plots of the EP and ENB polymers. The curve of the ENB polymer lies at the right side of that of EP polymer; this indicates that ENB polymer contains more gel than the EP polymer.

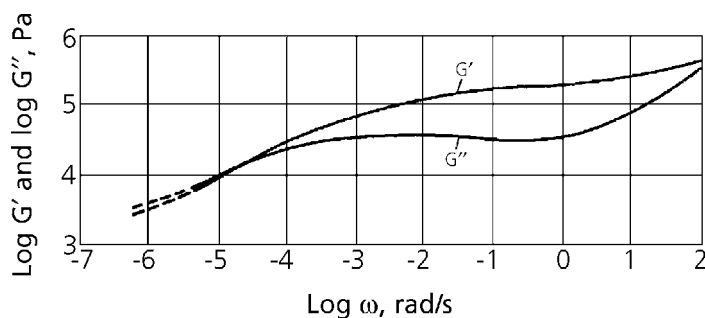


Figure 6.60 Storage and loss modulus as functions of angular frequency. EP ACM data reduced to 25 °C.

Reprinted with permission from N. Nakajima, R. A. Miller and E. R. Harrell, International Polymer Processing, 1987, 2, 2, 87. Copyright 1987, Hanser Publishers.

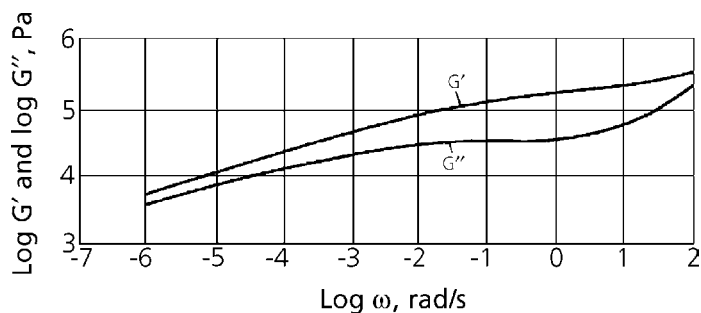


Figure 6.61 Storage and loss modulus as functions of angular frequency. ENB ACM data reduced to 25 °C.

Reprinted with permission from N. Nakajima, R. A. Miller and E. R. Harrell, International Polymer Processing, 1987, 2, 2, 87. Copyright 1987, Hanser Publishers.

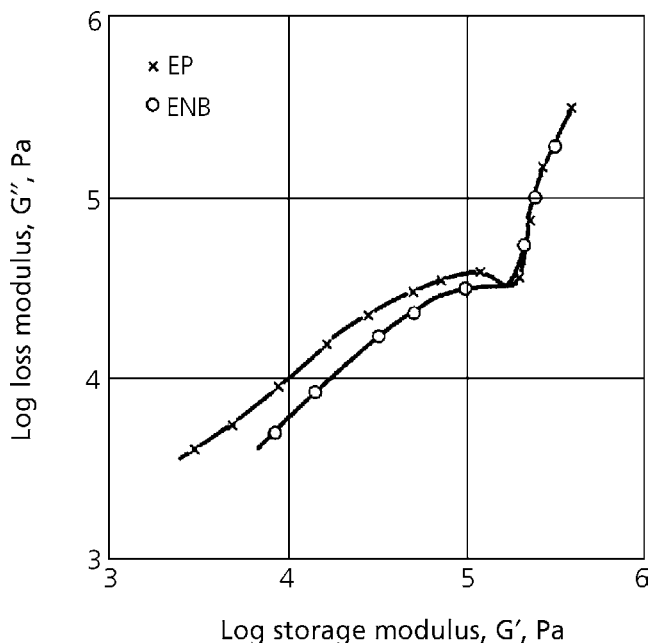


Figure 6.62 Modified Cole-Cole plots of EP and ENB ACM.

Reprinted with permission from N. Nakajima, R. A. Miller and E. R. Harrell, International Polymer Processing, 1987, 2, 2, 87. Copyright 1987, Hanser Publishers.

The tensile stress-strain data obtained at the previously mentioned four deformation rates have been converted to viscosity as a function of $(1/\alpha t)$. The data are presented in Figures 6.63 and 6.64, as $(\eta_T/3)$. The data points do not fall on one curve for the EP polymer, except for the shorter time range, at the right hand side of the figure. The deviations are systematic in that a higher deformation rate gives a higher viscosity. The difference appears to increase for the longer time, at the left hand side of the figure.

With the ENB polymer the data points fall on one curve, although some deviation of points similar to that of the EP polymer occurs. It can be concluded that the strain-time correspondence principle applies approximately to this sample. From the preceding argument, the gel particles in the ENB polymer must be microgels. On the other hand the EP polymer appears to contain long branching and macrogel.

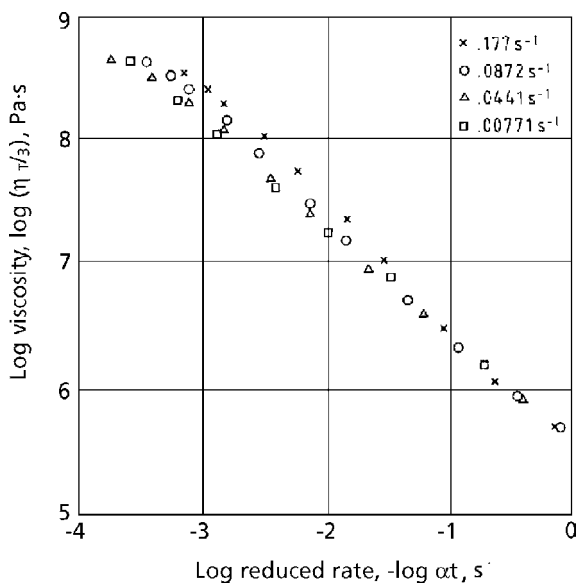


Figure 6.63 Viscosity evaluated from tensile stress-strain measurements; no formation of master curve, showing inapplicability of strain-time correspondence principle, EP ACM.

Reprinted with permission from N. Nakajima, R. A. Miller and E. R. Harrell, *International Polymer Processing*, 1987, 2, 2, 87. Copyright 1987, Hanser Publishers.

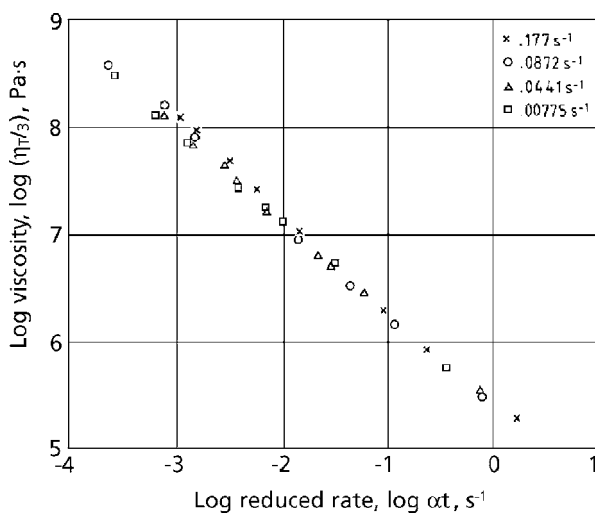


Figure 6.64 Viscosity evaluated from tensile stress-strain measurements; formation of master curve through application of strain-time correspondence principle, ENB ACM.

Reprinted with permission from N. Nakajima, R. A. Miller and E. R. Harrell, *International Polymer Processing*, 1987, 2, 2, 87. Copyright 1987, Hanser Publishers.

In Figure 6.65 the data of Figure 6.63 and 6.64 are plotted as modulus-reduced time ($1/\alpha t$) curves. The data had been interpolated at fixed extension ratios of $\alpha = 2, 4$, and 6. With the EP polymer the modulus data do not fall on one curve so that the strain-time correspondence does not apply. The modulus tends to be higher at the higher extension ratio, indicating strain-hardening. Therefore, the EP sample contains long branching and macrogel. On the other hand with the ENB polymer the modulus is independent of the extension ratio and a function of reduced time only. This means that the gel contained in this polymer is microgel.

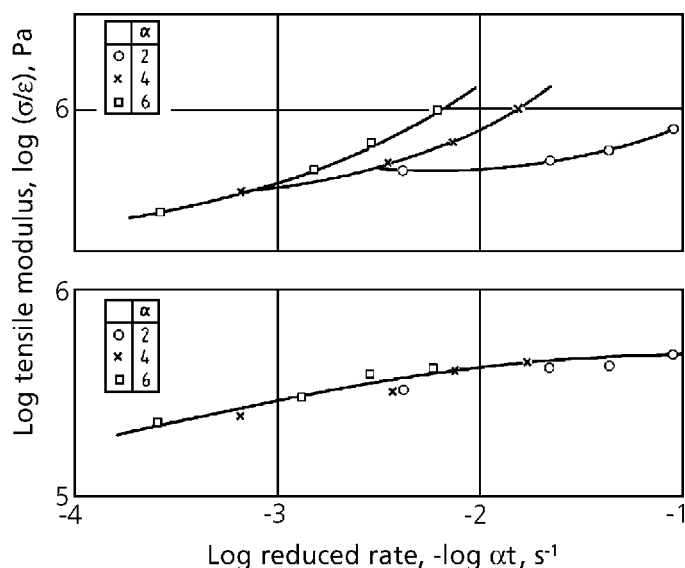


Figure 6.65 Modulus at equal strain observed at different deformation rates plotted as function of reduced time; strain hardening for EP sample (above) and no strain hardening for ENB sample (below).

Reprinted with permission from N. Nakajima, R. A. Miller and E. R. Harrell, *International Polymer Processing*, 1987, 2, 2, 87. Copyright 1987, Hanser Publishers.

- Discussion
- Mill processability and viscoelastic properties

Figure 6.66 (left and right) are photographs, illustrating the major differences in processability.

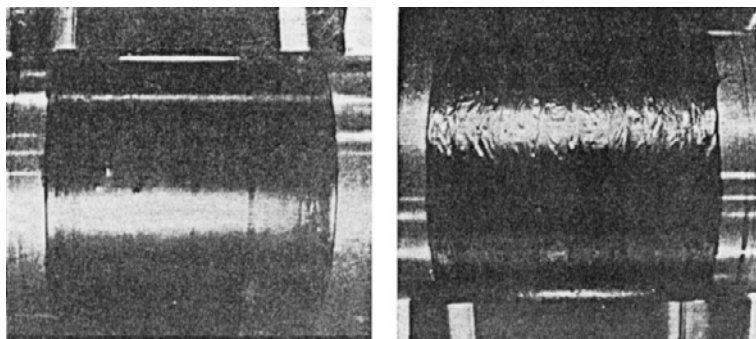


Figure 6.66 Banding characteristics of EP (right) and EMB (left) polyethacrylate at 150 °C.

Reprinted with permission from N. Nakajima, R. A. Miller and E. R. Harrell, International Polymer Processing, 1987, 2, 2, 87. Copyright 1987, Hanser Publishers.

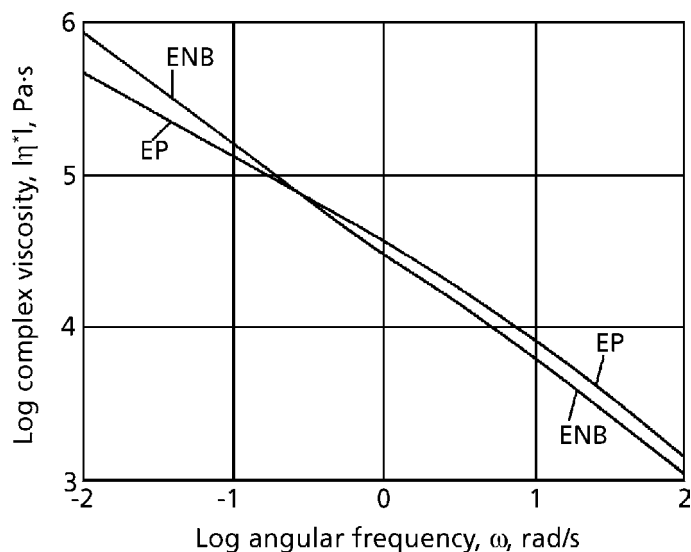


Figure 6.67 Complex viscosity-angular frequency curves of EP and ENB at 150 °C.

Reprinted with permission from N. Nakajima, R. A. Miller and E. R. Harrell, International Polymer Processing, 1987, 2, 2, 87. Copyright 1987, Hanser Publishers.

Whereas, the ENB polymer formed a smooth band around the roll and presented no problem in incorporating carbon black, the EP polymer became sticky and partially transferred into the backroll. There is a clear difference in the mill processability [28]. The ENB polymer exhibited Region II behaviour, which was a highly extensible, elastic state and best suited for mill processing. On the other hand the EP polymer was in Region IV, which was a flow state like a plastic melt. The relative difference in the behaviour may be understood by comparing the data of Figures 6.60 and 6.61 at the lower end of the frequency. Also, the same data at 150 °C are reproduced as the complex viscosity, $|\eta^*|$ as a function of ω , see Figure 6.67. At the lower frequency the viscosity of the EP polymer is lower than that of the ENB polymer. It should be remembered that polyethylacrylate polymer has 73% of its MW in the pendent, ester group [36]. Therefore, it is a relatively short chain for a given MW, with a larger cross-section compared to diene-rubbers, for example. This makes the polymer readily go to the molten state, when the temperature increases. The presence of microgel is known to introduce long relaxation times [38] such that the above undesirable tendency may be overcome. These results of the mill processability depend upon the temperature and the deformation rate; a higher rate corresponds to a lower temperature. Since our mill does not have a precise temperature control, the first batch starts at a lower temperature. The mill-mixing was conducted on different days; one day ENB was milled first and then EP. On another day it was in the reverse order. Although the EP polymer became sticky in both cases, it was less sticky when started with a colder mill.

- *Mechanisms of gel formation*

An inherent tendency for the polyethylacrylate to form long branching and gel has already been discussed in Section 1.1.6. In addition, the data of Table 6.7 show that the EP polymer crosslinked during pressing at 160 °C for 20 minutes. The gel content increased from 9.4 to 15.9%. This must have contributed to the strain-hardening tendency shown in Figure 6.65.

In the polymerisation of the ENB polymer, ENB is copolymerised to give a crosslinkable site. Since ENB is a difunctional monomer, it is hoped that only one functional group is incorporated into polymer chain. However, there must be a finite probability that the second functional group also becomes incorporated in the chain. This reaction leads to the microgel formation.

- *Temperature dependence of viscoelastic property*

The temperature shift factors found in shifting the observed curves of G' and G'' are given in Table 6.8. For the accuracy of superposition, the curves of G' and G'' are shifted together. The time shift factor, a_T and modulus shift factor, β_T are both based on 25 °C, $T_0 = 298$ K. The WLF constants [6], C_1 and C_2 are also given in Table 6.8:

$$-\log a_T = \frac{C_1(T - T_0)}{C_2 + (T - T_0)} \quad (6.40)$$

As far as the time-shift factor, a_T , is concerned, the EP polymer has a higher temperature-dependence, compared to the ENB polymer. This difference is apparent in the C_2 values, C_1 values being approximately equal. This result is similar to the temperature dependence of branched EPDM and linear EPM elastomers [39], where the branched elastomer had a higher temperature-dependence.

Table 6.8 Temperature Dependence of Viscoelastic Properties					
Sample	Temperature °C	a_T	β_T	C_1	C_2
EP	25	1.0	1.0	10.0	160
	60	1.7×10^{-2}	0.86		
	100	6.2×10^{-4}	0.82		
	150	6.3×10^{-5}	0.82		
ENB	25	1.0	1.0	11.4	227
	60	3.2×10^{-2}	0.92		
	100	1.2×10^{-3}	0.85		
	150	1.4×10^{-4}	0.83		

However, the present case is more complicated because the EP sample contains macrogel and the ENB sample contains microgel. Therefore, we cannot readily draw an analogy to the result of the previous study.

The modulus shift, β_T , is relatively small and subject to a proportionally large error. However, the shift is required for the superposition. This is in contrast to previous work with EPM and EPDM elastomers where such a shift was not required. The value of β_T decreases with increasing temperature; the extent of decrease is similar to what is expected from the theory, $\rho_0 T_0 / \rho T$. However, this subject is not pursued any further, since it is somewhat outside the scope of the present study.

6.8 Linear viscoelasticity

The linear viscoelasticity is a well established science and textbooks are available for understanding theories and practices. Therefore, no review of the subject will be made here. However, it is appropriate to make comments on the importance of linear

viscoelasticity where (i) it has direct relevance to mixing of rubber and (ii) it provides background for understanding rubber behaviour during mixing.

6.8.1 Linear viscoelasticity and mixing of rubber

As has been explained, mixing of rubber involves large deformation and fracture. In the former, non-linear viscoelasticity plays the key role. However, in limited cases linear viscoelastic behaviour also plays a key role. For example, the magnitude of shear storage modulus G' at the lower frequencies is related to the mill-processability in determining the initial reaction of rubber when it touches the mill-roll. That is, the flow state, rubbery state or rubber-glass transition defined by linear viscoelastic measurements at small deformation provides the practical information. After touching the mill-roll whether or not the rubber stretches and makes a tight band depends upon the non-linear viscoelastic property and fracture characteristics. An exception to this is that some rubber exhibits linear viscoelastic behaviour at a large deformation. Such rubber apparently retains the same internal structure (the arrangement of chains) even after stretching. Otherwise, modulus would change with strain, i.e., nonlinear behaviour.

The exact mechanism of how the linear behaviour is maintained in the large deformation is not known and is the subject of future research.

Another importance of linear viscoelasticity is that it provides a reference for non-linear behaviour; that is, the latter is expressed as a deviation from the former with use of appropriate parameters. First is the universal parameter, the elongation ratio, α , which reduces the time-scale of nonlinear behaviour to that of linear behaviour. Next is the modulus shift factor, $\Gamma(\alpha)$, which indicates the degree of strain-hardening or strain-softening. Finally, comparison of linearised elongation data with that of shear data indicates, if they disagree, the presence of strain-induced crystallisation or strain-induced association. All these deviations from linearity are related to the structure of rubber.

Thus far, a considerable variety of gum rubbers have been investigated and the characterisation scheme defined in this book is satisfactory. However, the applicability of the scheme is limited to the behaviour where strain-dependence and time-dependence are separable.

6.8.2 Relaxation time and its distribution

In order to relate viscoelasticity to processability, it helps to understand the concept of relaxation time. The definition of relaxation time customarily uses a spring and dashpot

for illustration. However, a definition is given here without using the spring and dashpot model.

Starting with a situation, where a stimulus is given to a system to excite it, the extent of the excitation is expressed by C^* . If the system is allowed to return to the ground state spontaneously, the rate $-dC^*/dt$ is proportional to the extent of excitation, C^* .

$$-dC^*/dt = kC^* \quad (6.41)$$

The integration of this equation gives a well-known equation,

$$C^* = C_0^* e^{-kt} \quad (6.42)$$

where C_0^* is the value of C^* at $t = 0$.

This equation is for the first order reaction in chemical kinetics.

It is also the equation for the decay of radioisotopes in physics.

In viscoelasticity

$$k = 1/\lambda \quad (6.43)$$

where λ is the relaxation time.

In the field of viscoelasticity there is 'retardation time' and relaxation time. Qualitatively these terms may be understood by analogy to human behaviour.

Suppose the reader has played tennis with his friend at lunch break and just returned to his work. After changing his clothes, he immediately resumes his work. His friend keeps talking about tennis and cannot go back to work. Which one of them has a longer relaxation time is obvious.

On a fine day at the weekend a reader invites his friend for a hike. He is ready to go but his friend is taking a long time in preparing for the hike. Which one of them has the longer retardation time is obvious.

In science, relaxation time and retardation time are quantitatively defined. In the viscoelasticity of polymers, the relaxation time is in general not a constant but it has a broad distribution. The retardation time also has a broad distribution. In linear viscoelasticity the distribution of relaxation time is shown in a stress relaxation experiment. The distribution of retardation time is shown by a creep experiment.

The distribution of relaxation time and that of retardation time are quantitatively related. Also, the result from any linear viscoelastic experiment is quantitatively related to distribution of relaxation or retardation time. Therefore, from the result of one type of linear viscoelastic measurement, the data of any other type of measurement can be calculated, provided the data are available for a wide range of time scales. For example, dynamic shear storage modulus, $G'(\omega)$ and dynamic shear loss modulus, $G''(\omega)$, may be calculated from relaxation modulus, $G(t)$. The method of calculation is described in textbooks [6] and outside of scope of this book. The importance here is to recognise that the distribution of the relaxation time is related to every data of linear viscoelasticity.

Accordingly, 'response time' or 'material time' is used to include both relaxation time and retardation time. Also, relaxation time is used somewhat loosely to represent both relaxation and retardation time for explaining observed phenomena. For discussing processability, it includes nonlinear viscoelasticity and the use of relaxation time tends not to be rigorous in the quantitative sense.

In the foregoing discussion the relaxation time is used in a relative sense invoking only long or short relaxation times.

In equation (6.41) for the chemical reaction, C^* is the concentration of the reactant. In radioisotope chemistry, the identity of the isotope is known. On the other hand in viscoelasticity, a material exhibiting certain relaxation time is often not clearly identified. Considering of the distribution of relaxation time, what is the counterpart of the distribution in material? Although much of this relationship is the subject of current and future studies, a general statement may be made as follows: for linear polymer chains, the size of the molecule and the relaxation time are directly related. However, the relaxation time of a given polymer chain is not only dependent on its size but also on its environment. For monodispersed polymers, when the MW is smaller than the entanglement coupling distance, Me , and when it is larger than Me , the environmental effect is completely different. For the latter case the environmental effect is called entanglement. For a molecule larger than Me , a local motion of a chain segment, which is smaller than Me , is also present.

For a given polymer molecule, its motion may be divided into relatively fast motions of the segments which are smaller than Me and relatively slower motions of the whole chain, which is larger than Me . This interpretation may be expanded to include polymers having MW distribution. Considering the whole polymer there must be a relationship between the longest relaxation time (terminal relaxation time) and its MW. An example is the relationship between low shear Newtonian viscosity, η_0 , and MW. With commercial gum rubbers, η_0 is observed only with low MW polymer or a polymer whose MW distribution lacks the high MW tail. Nevertheless, η_0 will be considered for a moment.

The presence of long branches is very common in gum rubbers and the branch pattern varies widely. For simplicity, a 'star-branched' polymer will be taken as an example. The reader should be aware that this type of model polymer does not represent all other types of branched polymers. Nevertheless, some common features of the branched polymers may be extracted by examining these model polymers.

Figure 6.68 presents plots of η_0 against weight average MW, \overline{M}_w for linear, 3 arm-star and 4 arm-star polymers [40].

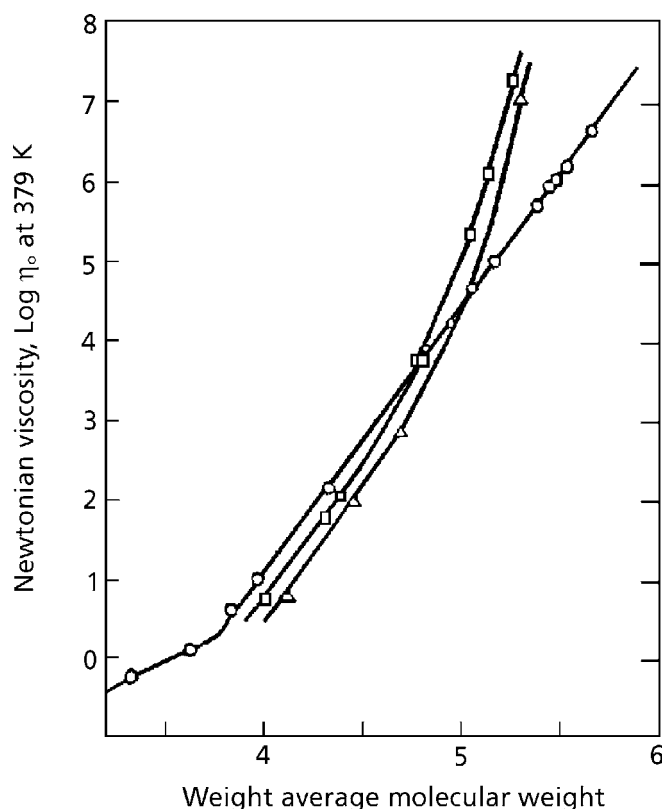


Figure 6.68 Relationship between Newtonian viscosity and MW.

- : Linear molecule
- : Tribranched molecule
- △: Tetrabranched molecule

Reprinted from G. Kraus and J. T. Gruver, *Journal of Polymer Science*, 1965, A3, 1, 105.
Copyright 1965, John Wiley & Sons, Inc. Reprinted by permission of John Wiley & Sons, Inc.

They are BRs prepared through anionic polymerisation. Compared at a fixed MW, the branched polymer has a lower η_0 below certain MW and a higher η_0 above certain MW.

The relaxation time apparently depends upon not only the size of molecule but also its shape, which is branching in this case. Compared at the same size, the branching makes relaxation time shorter below certain branch length and longer above this branch length. The critical branch length is 3 to 4 times of Me [41, 42, 43, 44]. Above this crossover MW, the long branch enhanced viscosity.

With a branched polymer exhibiting viscosity enhancement, the extent of the enhancement decreases with increasing shear rate, eventually crossing over the viscosity curve of the linear polymer. That is, at the high shear rate the viscosity is reduced by the presence of long branches. The commercial gum rubbers have branch patterns quite different from the model star polymers. However, often branching is present in the high MW fraction so that the viscosity enhancement at the low shear rates and viscosity reduction at the high shear rates are common observations. This crossover behaviour is also observable in the frequency dependence of the dynamic viscosity, see Figure 6.13 [32].

The long relaxation times introduced by the long branches of commercial gum rubbers have significant influence, even though the amount of the branched fraction may be very small. In the characterisation using dilute solution methods sometimes the branched fraction is filtered off. Then, the interpretation of the processability becomes very difficult.

The presence of gel molecules may be interpreted as a part of the size distribution. The effect of gel is to introduce a very long relaxation time. It exhibits viscosity enhancement at the low shear rate and viscosity reduction at the high shear rate. This occurs with both macrogel and microgel. The details of this mechanism are subjects for future study.

When a polymer blend has island-and-sea morphology, the deformation of the island has a very long relaxation time. The viscosity enhancement was observed at the low shear rate [45].

6.8.3 Linear viscoelasticity as a conceptual background for the mixing of rubber

Different deformational measurements are used to obtain linear viscoelastic data. It may be in simple shear or in elongation. However, the behaviour of rubber during

mixing is neither simple shear nor elongation. Also, in the laboratory measurements, conditions are imposed to be a constant temperature, a constant rate of deformation, a constant frequency, a constant strain or a constant stress over a period of time. Neither one of these conditions are met by the behaviour of rubber during mixing. Then, what is the use of these idealised measurements?

There are two important answers to satisfy the question: one is that the information obtained for a given gum rubber with the above measurements are all related and that from the result of one type of measurement, the result of any other type of measurement, can be calculated. The implication is that if one type of measurement is made then everything about a given gum rubber is known with respect to its linear viscoelastic behaviour. The information is, of course, limited to the range of time scale and the range of temperature of observation.

The other importance is the additivity of the memory. That is, using shear stress relaxation as an example, the cumulative memory of stresses imposed at different times may be calculated with a theory of Boltzmann's superposition principle.

The implication of these two statements is profound. When the separability of time and strain holds for a given gum rubber, subsequent linearisation of the data enables one to describe the behaviour of a gum rubber under any situation, at least in principle. This means that with the understanding of linear viscoelasticity plus the parameters for linearisation, there is adequate information for diagnosing processing problems.

6.8.4 Viscoelasticity and memory

The concept of memory is well accepted today. Memory tapes, memory discs and other memory storage devices are an integral part of our society. However, they are usually either electromagnetic or optical devices. Actually material possesses the ability to retain memories of various kinds; it is also capable of losing memory. In the field of viscoelasticity, the memory appears as a change of shape. If a body is elastic but non-viscous, the memory is retained while a stress is imposed; upon removal of the stress, the memory recovers by 100% and the shape returns to the original. Then, the memory of the deformation is completely gone. With a viscoelastic body, it is not as simple. When a constant stress is imposed, the deformation is not instant but increases with time; this phenomenon is called creep. When the stress is removed, the memory does not recover instantly. It does not necessarily return to the original shape.

When a constant strain is imposed, the stress decreases with time. This is called stress relaxation. The manner of the relaxing stress is a manifestation of the memory loss.

Creep and stress relaxation are model experiments. The stress-strain relations in polymer processing are much more complex. However, the memory phenomena are observed frequently. A typical example is the extrudate swell [46]. In the mixing of rubber it appears as the mill-shrinkage. When the rubber is sheeted out of the mill roll, the thickness increases, and the width and the length decrease. The extent of the change depends upon the material and therefore, the mill-shrinkage has been used as a measure of the material characteristics. When the manner of the memory-loss in the stress-relaxation is considered, there are memories lost in a short time and those retained for a long time. The former memory arises from short relaxation times and the latter from the long relaxation times. The polymer has a distribution of relaxation times and the memory phenomenon is their manifestation.

The relaxation time, λ , is expressed as the ratio of viscosity, η , and elastic (shear) modulus, G ,

$$\lambda = \eta/G \quad (6.44)$$

When a system has a single relaxation time, this relationship is easy to understand. When there is a distribution of relaxation times, the meaning of η and G , is not very simple. Therefore, instead of separating the relaxation time into η and G , the relaxation time itself will be used to describe material behaviour.

In the rubber processing neither stress nor strain remains constant over time. Therefore, creep or stress relaxation is not an appropriate model. On the other hand a very complicated stress-strain history is difficult to interpret. A simpler model which offers some insight into processability may be found in transient behaviour. One example is a stress-growth under a constant rate of deformation and observation of stress relaxation. To be realistic, the strain must be large and the behaviour must be in nonlinear viscoelasticity. The experiments may be carried out with a rotational rheometer but they are restricted to low rates of deformation, because otherwise rubber slips at the rheometer interface [47, 48].

Figure 6.69 shows examples of stress history.

Curve 3 is the stress relaxation from the ‘instantaneous’ deformation, which retains 100% memory at $t = 0$ and exhibits the memory-loss thereafter.

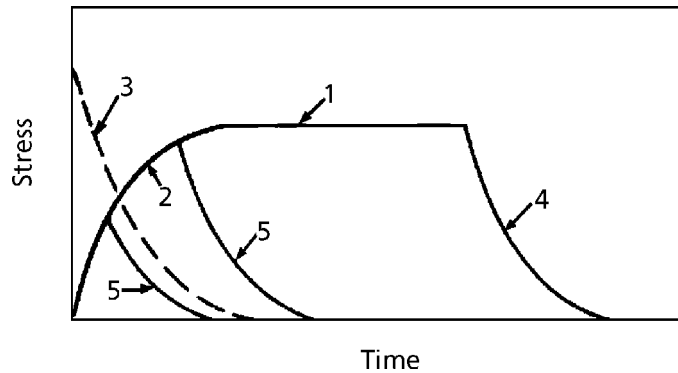


Figure 6.69 Schematic illustration of types of experiments:

- 1) steady state
- 2) stress-rise
- 3) stress relaxation after instantaneous deformation
- 4) stress relaxation after the cessation of flow
- 5) stress relaxation after constant rate of deformation

*Reprinted from N. Nakajima and E. R. Harrell, Journal of Rheology, 1983, 27, 3, 241.
Copyright 1983, The Society of Rheology. Reprinted by permission of John Wiley & Sons, Inc.*

Curve 2 shows stress-growth with low rates of deformation, during which a part of memory is lost. If the deformation is stopped and the strain is held constant, the relaxation shown by curve 5 is observed. When the deformation is carried to the steady state condition, the stress becomes constant, Curve 1. It means that stress is proportional to strain rate and no longer increases with deformation. Curve 4 is the relaxation from the steady state. It is a manifestation of the steady state memory and its dissipation with time. When the relaxation curves, 3, 4 and 5, are expressed as relaxation modulus-time curves, see Figure 6.70, larger differences are observed in the shorter times, but for the longer times the curves merge.

This means that the memory associated with short relaxation times is lost during the imposition of deformation but the memory associated with long relaxation times is retained. Understanding the meaning of the experiment helps interpretation of memory phenomena in processing.

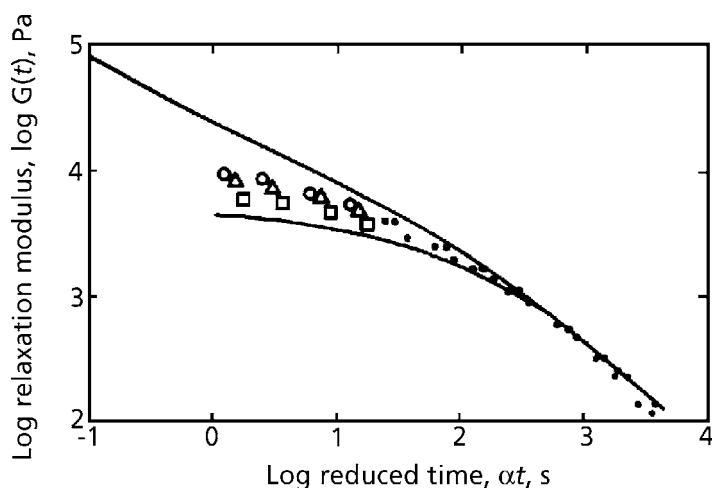


Figure 6.70 Relaxation modulus after constant rate of deformation (●) compared with that after instantaneous deformation (upper curve) and that after cessation of flow (lower curve) for BN-1 sample. Rate of deformation = $0.049\text{--}0.050\text{ s}^{-1}$ and strain = 0.405 (○), 0.785 (△) and 1.205 (□).

Reprinted with permission from N. Nakajima and E. R. Harrell, Journal of Rheology, 1983, 27, 3, 241. Copyright 1983, The Society of Rheology. Reprinted by permission of John Wiley & Sons, Inc.

One drawback of the previous experiment is the slow rate of deformation. In order to match the deformation rate to that in processing, a capillary rheometer may be used. A memory introduced in the deformation at the capillary entrance corresponds to curve 2. Once a material is in the capillary the behaviour is like curve 1, except that some relaxation takes place during the flow through capillary. The recovery of memory appears as the extrudate swell, which is not stress relaxation but like a creep recovery. Because some relaxation takes place during the flow, the recovery depends upon the residence time in capillary which is proportioned to the L/D of the capillary. The higher shear rate results in a shorter residence time in capillary. Therefore less memory is lost and the extrudate swell is higher.

Experiments described in this section concern transient behaviour. Although they are model experiments, they are a closer simulation to the deformational behaviour of gum rubber during mixing than the use of steady state viscosity. The analyses of the transient behaviour with uses of relaxation times, and the interpretation of the memory are a useful way for diagnosing mixing behaviour.

References

1. I. M. Ward, *Mechanical Properties of Solid Polymers*, 2nd Edition, Wiley-Interscience, New York, 1983.
2. R. S. Rivlin, in *Rheology*, Vol. 1, Ed., F. R. Eirich, Academic Press, New York, 1956, Chapter 10.
3. M. Mooney, *Journal of Applied Physics*, 1940, **11**, 582.
4. K. C. Valanis and R. F. Landel, *Journal of Applied Physics*, 1967, **38**, 2997.
5. R. W. Ogden, P. Chadwick and E. W. Hadden, *Quarterly Journal of Mechanics and Applied Mathematics*, 1973, **26**, 23.
6. J. D. Ferry, *Viscoelastic Properties of Polymers*, 3rd Edition, Wiley, New York, 1980.
7. T. L. Smith, *Transactions of the Society of Rheology*, 1962, **6**, 61.
8. R. A. Schapery, *Polymer Engineering Science*, 1969, **9**, 4, 295.
9. B. Bernstein and A. Shokooh, *Journal of Rheology*, 1980, **24**, 189.
10. N. Nakajima and E. R. Harrell, *Rubber Chemistry and Technology*, 1980, **53**, 1, 14.
11. N. Nakajima, J. J. Scobbo, Jr., and E. R. Harrell, *Rubber Chemistry and Technology*, 1987, **60**, 742.
12. N. Nakajima, *Journal of Non-Newtonian Fluid Mechanics*, 1983, **12**, 349.
13. P. A. Small, *Advances in Polymer Science*, 1975, **18**, 1.
14. ASTM D 1646-96a
Standard Test Methods for Rubber - Viscosity, Stress Relaxation, and Pre-Vulcanisation Characteristics (Mooney Viscometer).
15. N. Nakajima and E. A. Collins, *Rubber Chemistry and Technology*, 1974, **47**, 2, 333.
16. M. Mooney and W. E. Wolstenholme, *Journal of Applied Physics*, 1954, **25**, 1098.
17. N. Nakajima and E. R. Harrell, *Rubber Chemistry and Technology*, 1979, **52**, 1, 9.

18. K. Ninomiya, S. Kusamizu, E. Maekawa and G. Yasuda, *Progress in Polymer Science in Japan*, Vol. 1, Eds., M. Imoto and S. Onogi, Kodansha, Tokyo, 1971, p.377.
19. N. Nakajima and E. R. Harrell, in *Current Topics in Polymer Science*, Vol. II, Eds., R. M. Ottenbrite, L. A. Utracki and S. Inoue, Hanser Publications, New York, 1987, p.150.
20. ASTM D 3616-95.
Standard Test Method for Rubber, Raw - Determination of Gel, Swelling Index, and Dilute Solution Viscosity.
21. N. Nakajima, E. R. Harrell, P. R. Kumler, D. A. Seil and A. H. Jorgensen, *Advances in Polymer Technology*, 1984, **4**, 3/4, 267.
22. N. Nakajima, C. D. Huang, J. J. Scobbo, Jr., and W. J. Shieh, *Rubber Chemistry and Technology*, 1989, **62**, 2, 343.
23. N. Nakajima, D. Erbe, A. Maeda and H. Yamazaki, *Rubber World*, 1991, **205**, 2, 33.
24. N. Nakajima and E. R. Harrell, *Rubber Chemistry and Technology*, 1983, **56**, 5, 1019.
25. E. R. Harrell and N. Nakajima, *Journal of Applied Polymer Science*, 1984, **29**, 3, 995.
26. N. Nakajima, M. H. Chu and R. Babrowicz, *Rubber Chemistry and Technology*, 1990, **63**, 4, 624.
27. N. Nakajima, W. J. Shieh and Z. G. Wang, *International Polymer Processing*, 1991, **6**, 4, 290.
28. N. Tokita and J. L. White, *Journal of Applied Polymer Science*, 1966, **10**, 7, 1011.
29. W. H. Whittington and M. E. Woods, Presented at the 100th Meeting of the ACS Rubber Division, Cleveland, OH, Fall 1971, Paper No.38.
30. N. Nakajima and Y. Yamaguchi, *Journal of Applied Polymer Science*, 1996, **61**, 9, 1525.
31. ASTM D412-98a
Standard Test Methods for Vulcanised Rubber and Thermoplastic Rubbers and Thermoplastic Elastomers - Tension

32. N. Nakajima and E. R. Harrell, *Rubber Chemistry and Technology*, 1980, **53**, 1, 14.
33. N. Nakajima and Y. Yamaguchi, *Journal of Applied Polymer Science*, 1996, **62**, 13, 2329.
34. M. Takayanagi, Presented at the 19th Annual Meeting of the International Institute of Synthetic Rubber Producers, Inc., Hong Kong, 1978, Paper No.21
35. N. Nakajima and Y. Yamaguchi, *Journal of Applied Polymer Science*, 1997, **65**, 10, 1995.
36. R. D. DeMarco, *Rubber Chemistry and Technology*, 1979, **52**, 1, 173.
37. *Encyclopedia of Composite Materials and Compounds*, Ed., M. Grayson, Wiley, New York, 1983.
38. N. Nakajima and E. A. Collins, *Journal of Rheology*, 1978, **22**, 5, 547.
39. N. Nakajima and E. R. Harrell, *Journal of Rheology*, 1982, **26**, 5, 427.
40. G. Kraus and J. T. Gruver, *Journal of Polymer Science*, 1965, **A3**, 105.
41. V. R. Raju, G. G. Smith, G. Marin, J. R. Knox and W. W. Graessley, *Journal of Polymer Science: Polymer Physics*, 1979, **17**, 7, 1183.
42. W. E. Rochefort, G. G. Smith, H. Rachapudy, V. R. Raju and W. W. Graessley, *Journal of Polymer Science: Polymer Physics*, 1979, **17**, 7, 1197.
43. H. Rachapudy, G. G. Smith, V. R. Raju and W. W. Graessley, *Journal of Polymer Science: Polymer Physics*, 1979, **17**, 7, 1211.
44. V. R. Raju, H. Rachapudy and W. W. Graessley, *Journal of Polymer Science: Polymer Physics*, 1979, **17**, 7, 1223.
45. N. Nakajima and P. S. L. Wong, *Journal of Applied Polymer Science*, 1965, **9**, 9, 3141.
46. N. Nakajima, *Journal of the Rheology Society, Japan*, 1990, **18**, 5.
47. N. Nakajima and E. R. Harrell, *Journal of Rheology*, 1983, **27**, 3, 241.
48. N. Nakajima and E. R. Harrell, *Journal of Rheology*, 1986, **30**, 2, 383.

